

## Strategies for the use and interpretation of functionalized reverse osmosis membranes with improved antifouling and anti-scaling properties for the desalination process

Dana A. Da'na, Nadiene Salleha Mohd Nawi, Farah I. Sangor, Mohammad Y. Ashfaq, Woei Jye Lau, Mohammad A. Al-Ghouti

### Item type

Journal Contribution

### Terms of use

This work is licensed under a [CC BY 4.0](#) license

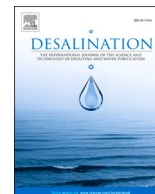
### This version is available at

[https://manara.qnl.qa/articles/journal\\_contribution/Strategies\\_for\\_the\\_use\\_and\\_interpretation\\_of\\_functionalized\\_reverse\\_osmosis\\_scaling\\_properties\\_for\\_the\\_desalination\\_process/28123589/1](https://manara.qnl.qa/articles/journal_contribution/Strategies_for_the_use_and_interpretation_of_functionalized_reverse_osmosis_scaling_properties_for_the_desalination_process/28123589/1)

Access the item on Manara for more information about usage details and recommended citation.

Posted on Manara – Qatar Research Repository on

2024-12-31



# Strategies for the use and interpretation of functionalized reverse osmosis membranes with improved antifouling and anti-scaling properties for the desalination process

Dana A. Da'na<sup>a</sup>, Nadiene Salleha Mohd Nawī<sup>b</sup>, Farah I. Sangor<sup>a</sup>, Mohammad Y. Ashfaq<sup>a</sup>, Woei Jye Lau<sup>b,\*</sup>, Mohammad A. Al-Ghouti<sup>a,\*</sup>

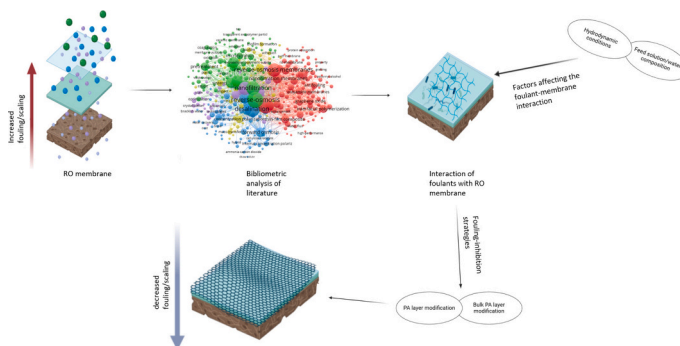
<sup>a</sup> Department of Biological and Environmental Sciences, College of Arts and Sciences, Qatar University, P.O. Box 2713, Doha, Qatar

<sup>b</sup> Advanced Membrane Technology Research Centre (AMTEC), Faculty of Chemical and Energy Engineering, Universiti Teknologi Malaysia, 81310 Johor Bahru, Johor, Malaysia

## HIGHLIGHTS

- This review provides a ten-year research overview on RO membrane fouling.
- It compares mitigating membrane fouling through surface coating and membrane fabrication.
- Membrane fouling occurs due to interactions between foulants and the membrane itself.
- Various materials like GO, CNT, and TiO<sub>2</sub> are used to modify RO membrane.

## GRAPHICAL ABSTRACT



## ARTICLE INFO

### Keywords

Reverse osmosis  
Biofouling  
Scaling  
Membrane fouling  
Nanomaterials  
Nanoparticles  
Bibliometric analysis

## ABSTRACT

Membrane technology significantly contributes to clean water production through industrial wastewater treatment or seawater desalination. The membrane fouling caused by the constituents of feedwater affects the performance of the reverse osmosis (RO) membrane by partially or completely blocking the membrane pores and increasing the system's operating cost. This review utilized bibliometric analysis to provide an overview of research conducted on RO membrane fouling during the past 10 years. The membrane-foulant and foulant-foulant interactions govern the phenomenon of membrane fouling, and therefore this review discusses these interactions in detail. Also, the materials used to inhibit membrane fouling through membrane surface coating or membrane fabrications are compared comprehensively.

\* Corresponding authors.

E-mail addresses: [lwoeijye@utm.my](mailto:lwoeijye@utm.my) (W.J. Lau), [mohammad.alghouti@qu.edu.qa](mailto:mohammad.alghouti@qu.edu.qa) (M.A. Al-Ghouti).

<https://doi.org/10.1016/j.desal.2024.118508>

Received 20 July 2024; Received in revised form 7 December 2024; Accepted 26 December 2024

Available online 31 December 2024

0011-9164/© 2025 The Authors. Published by Elsevier B.V. This is an open access article under the CC BY license (<http://creativecommons.org/licenses/by/4.0/>).

## 1. Introduction

In the last decade, economic growth and population expansion have caused a 600 % increase in global water demand [1]. Desalination is a promising method to overcome the water scarcity issue. According to Thu et al. [2], an efficient way to solve the increased demand for drinking water could be through increasing the desalination capacity worldwide from 2.9 billion m<sup>3</sup>/month to 13.6 billion m<sup>3</sup>/month as well as through promoting the use of treated wastewater from 1.6 billion m<sup>3</sup>/month to 4.0 billion m<sup>3</sup>/month. Thermal desalination techniques negatively affect the environment because of their high energy requirements, emissions of CO<sub>2</sub>, and the effect on aquatic life due to the disposal of warm brine water [3]. Therefore, with the development of appropriate polymer films in the 1960s, the membrane-based desalination technique became a practical commercial alternative to the conventional thermal desalination processes.

One of the most common membrane-based desalination techniques is reverse osmosis (RO) which can desalinate water with different salt levels by forcing the salty water to pass through the suitable membrane that holds most of the ions [4]. Based on the osmosis phenomenon, RO expels salts from water by the distinction of osmotic pressure between water and salty water. The physical process of RO has various advantages such as less energy and chemical demand, easy operation, as well as larger permeation flux [5]. In the past couple of decades, the popularity of RO processes in modern desalination has increased due to its superior performance compared to conventional thermal techniques and high product water standard, the technology has massively dominated the commercial desalination market [6].

RO membranes are vital components of the desalination process, playing a pivotal role in the efficient separation of salt and other impurities from water. Their construction using thin polymeric films, such as cellulose acetate or polyamide, is driven by the desire for optimal membrane properties. These materials exhibit high permeability, rejection, flux, and mechanical stability, making them well-suited for the demands of desalination applications. However, the efficiency and performance of RO desalination are challenged by membrane fouling, a common issue associated with the process [7]. As a result, more energy is required to maintain the desired water production rate, increasing operational costs and enhancing environmental impacts. Similarly, scaling leads to reduced permeability and increased energy requirements to maintain a constant water production rate [8,9]. The properties of the RO membrane, such as surface charge, hydrophobicity, morphology, and material composition, influence fouling and scaling behaviors. Changes in operating conditions, such as temperature, pressure, and flow rate, can impact the deposition and adhesion of foulants and scaling precursors on the membrane surface. Moreover, the quality of feed water plays a crucial role, as it can contain suspended particles, colloids, dissolved organic matter, microorganisms, and dissolved ions, which can lead to membrane fouling and compromise its performance.

Consequently, the development of anti-fouling and anti-scaling RO membranes holds immense importance. Multiple studies have yielded significant breakthroughs in the field, offering promising solutions to the inherent fouling challenges associated with RO membrane-based desalination [10]. These research efforts have resulted in the development of highly efficient and advanced RO membranes that exhibit improved anti-fouling and anti-scaling properties achieved by improving the membrane materials and modification of its surface.

Our review contributes significantly to the field of antifouling strategies for RO membranes compared to existing literature. A more comprehensive investigation of biofouling, organic biofouling, and advanced nanocomposite materials, as well as highlighting the integration of advanced technologies and methodologies. Therefore, this review offers a more detailed and comprehensive discussion of the emerging materials emphasizing biofouling control methods that have not been fully covered in previous reviews. Furthermore, the novelty of our paper comes from the focus on the practical applications and

industrial applications compared to previous papers that focused on theoretical or lab-based discussions such as ([12,14] and [15]). Moreover, innovatively including bibliometric analysis for the evaluation of antifouling strategies for RO membrane distinguishes our paper and makes it more novel compared to the existing reviews that depend on qualitative assessments. Our quantitative framework ensures a clear understanding of the influential journals in the field as well as the research trends and key contributors which in turn helps in addressing the research gaps in this field.

This comprehensive review provides an overview of the RO membrane fouling research done in the literature during the past decade by utilizing bibliometrics and meta-analysis. This section helped to provide various insights into the literature in terms of the contribution of various countries, institutions, and authors towards RO membrane fouling research and highlighted the most frequently researched areas. Then, the review highlights the factors influencing membrane-foulant interaction targeting the membrane properties and hydrodynamic conditions. This paper also comprehensively discusses the performance of various organic, inorganic, and hybrid materials in inhibiting membrane fouling as reported in the literature.

## 2. Overview of RO membrane fouling research

### 2.1. Bibliometric analysis of the literature

The bibliometric analysis was conducted to investigate RO membrane fouling research. The analysis was conducted on January 17, 2024 for the research conducted in the last 10 years (2014–2023). The preliminary analysis was done on the selection of search terms to ensure that all relevant information is obtained from the Web of Science (WoS) database.

Hence, the data was collected using (“reverse osmosis” OR “RO”) AND (“\*foul\*” OR “\*scaling\*” OR “\*scalant\*”), and the dates were customized as 01/01/2014–31/12/2023. For the author’s co-authorship analysis, the number of documents of an author was restricted to 10, and 214 out of 12,585 authors met the threshold. For the organization’s co-authorship analysis, the minimum number of documents was kept at 20, 79 organizations out of 2806 met the threshold. Among 79 organizations, 3 were found to be not connected. The minimum number of documents for co-authorship analysis at countries level was done by restricting 20 documents per country. Following this criterion, out of 94 countries, 41 met the threshold. The keyword co-occurrence analysis was conducted using the web-based Biblioshiny platform under the Bibliometrix R package. The co-occurrence network was created using the Walktrap algorithm and ‘association’ was used as the normalization method [16]. The minimum number of nodes (representing keywords) was set at 125 and the size of the node was proportional to the number of times a keyword has appeared in the literature.

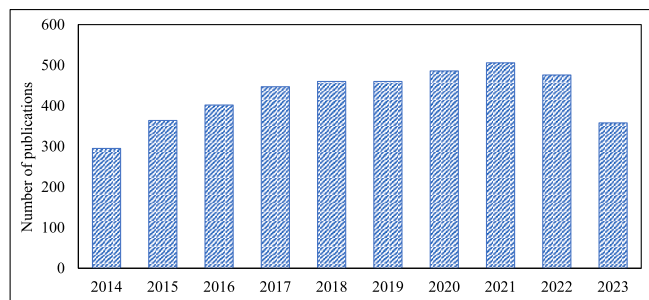


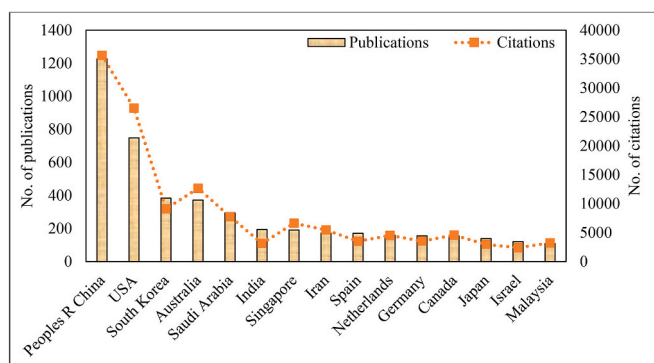
**Fig. 1.** The number of publications during the past 10 years in the field of RO membrane fouling.

## 2.2. Distribution of literature by year

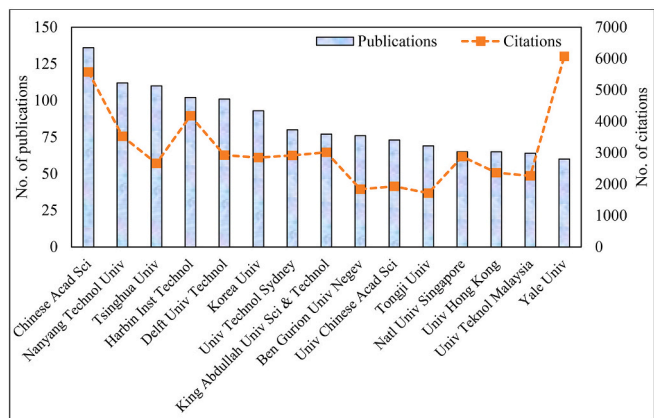
During the past decade, the number of papers published on RO membrane fouling research was 4254. From Fig. 1, it is evident that the number of documents published ranged from 295 (2014) to 506 (2021). The figure also shows that there has been a steady increase in several publications during the past 10 years.

## 2.3. Data analysis by countries, organizations, and authors

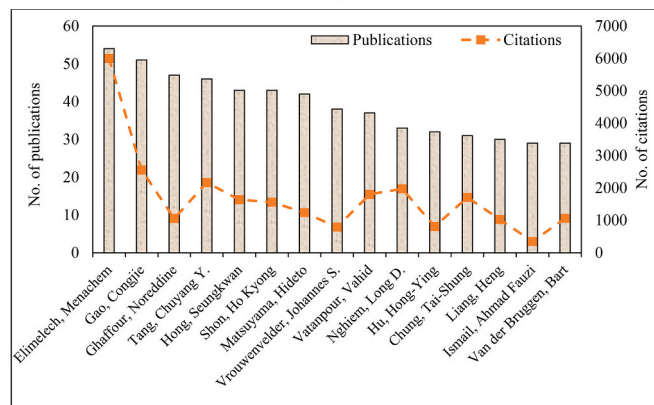
Fig. 2a shows the contribution of the top 15 countries in the field of RO membrane fouling. It is evident that China (1227 publications, 35,652 citations) and the USA (748 publications, 26,521 citations) have led the number of publications during the past 10 years in this area.



(a)



(b)



(c)

Fig. 2. Contribution of (a) countries, (b) institutes, and (c) authors to membrane fouling research during the last 10 years (2014–2023).

These countries are followed by South Korea (384 documents, 9111 citations), Australia (372 articles, 12,664 citations), and Saudi Arabia (294 publications, 7764 citations). Moreover, Fig. S1a shows countries' co-authorship analysis, resulting in 5 clusters. The red cluster consisted of 13 countries, among which the most notable ones were the People's Republic of China (1227 documents), Australia (372 documents), India (194 documents), and Japan (139 articles) showing their close collaboration between each other. The green cluster contained 10 countries, with the dominant contribution from Iran (172 documents), Canada (155 documents), Malaysia (109 documents), and Qatar (73 documents). The blue cluster comprising 7 countries showed a dominant contribution from Spain (171 articles), England (90 papers), France (87 documents), and Brazil (77 documents). The yellow cluster comprised 6 countries with dominant contributions from the Netherlands (159 articles), Germany (156 documents), Israel (120 papers), and Belgium (84 documents). Finally, the purple cluster containing 5 countries was dominated by the USA (748 documents), South Korea (384 documents), Saudi Arabia (294 documents), and Singapore (191 articles).

Fig. 2b shows the top 15 institutions that have contributed to the field of membrane fouling. Among them, the Chinese Academy of Sciences (136 publications, 5576 citations), Nanyang Technological University (112 documents, 3525 citations), Tsinghua University (110 publications, 2663 citations), Harbin Institute of Technology of China (102 research documents, 4181 citations), and Delft University of Technology of the Netherlands (101 articles, 2927 citations) are the top 5 universities with the highest number of publications during the last decade. Most of these are Chinese institutes showing the contribution of China in membrane fouling research. It was also noted that the Yale University of USA with just 60 publications has the maximum number of citations, i.e., 6075 demonstrating its impactful contribution to the discipline. Fig. S1b shows the institution's co-authorship analysis that resulted in 9 clusters of institutes based on their frequent collaborations.

The contribution of the top 15 authors is depicted in Fig. 2c. Among them, the top 5 authors who contributed the most are Elimelech, Menachem (54 documents, 5999 citations), Gao, Congjie (51 documents, 2555 citations), Ghaffour, Noreddine (47 documents, 1058 citations), Tang, Chuyang (46 documents, 2170 citations), and Hong, Seungkwan (43 documents, 1639 citations). Fig. S1c shows a total of 33 clusters which represents the number of research groups working on membrane fouling research and how they are segregated from each other.

## 2.4. Keyword co-occurrence analysis

The keyword co-occurrence analysis helps to understand the main research areas and how different concepts/factors of the given topic are studied together [17]. Fig. 3 shows the keyword co-occurrence network, and Table 1 summarizes the frequencies of the most commonly used keywords, and their centrality parameters with the main research themes (depicted in Fig. 3).

The keyword co-occurrence analysis resulted in 3 big clusters/themes. The red cluster was centered around the 'reverse osmosis' with a frequency, "F" of 955 (Table 1). Among the most related topics to reverse osmosis, were 'nanofiltration' (F = 431), 'desalination' (F = 322), and 'biofouling' (F = 311). Compared to 'biofouling', Fig. 3 shows that other types of fouling like 'scaling', 'organic fouling', 'colloidal fouling', and particularly 'combined fouling' are less studied. This can also be confirmed by high values of betweenness centrality and PageRank for biofouling as compared to the other types of fouling (Table 1). Under scaling, the most common scalants investigated are 'calcium carbonate', 'gypsum', and 'silica'.

The blue cluster is around the topic of 'fouling' with a total of 740 occurrences. The cluster reveals that 'forward osmosis' (F = 263), and 'ultrafiltration' (F = 197) are commonly studied and linked to 'fouling' research themes. Among the foulants, the most common are 'humic acid', 'natural organic matter', 'transparent exopolymer particles', 'alginate', and 'calcium'. The green cluster is related to 'anti-fouling' (F

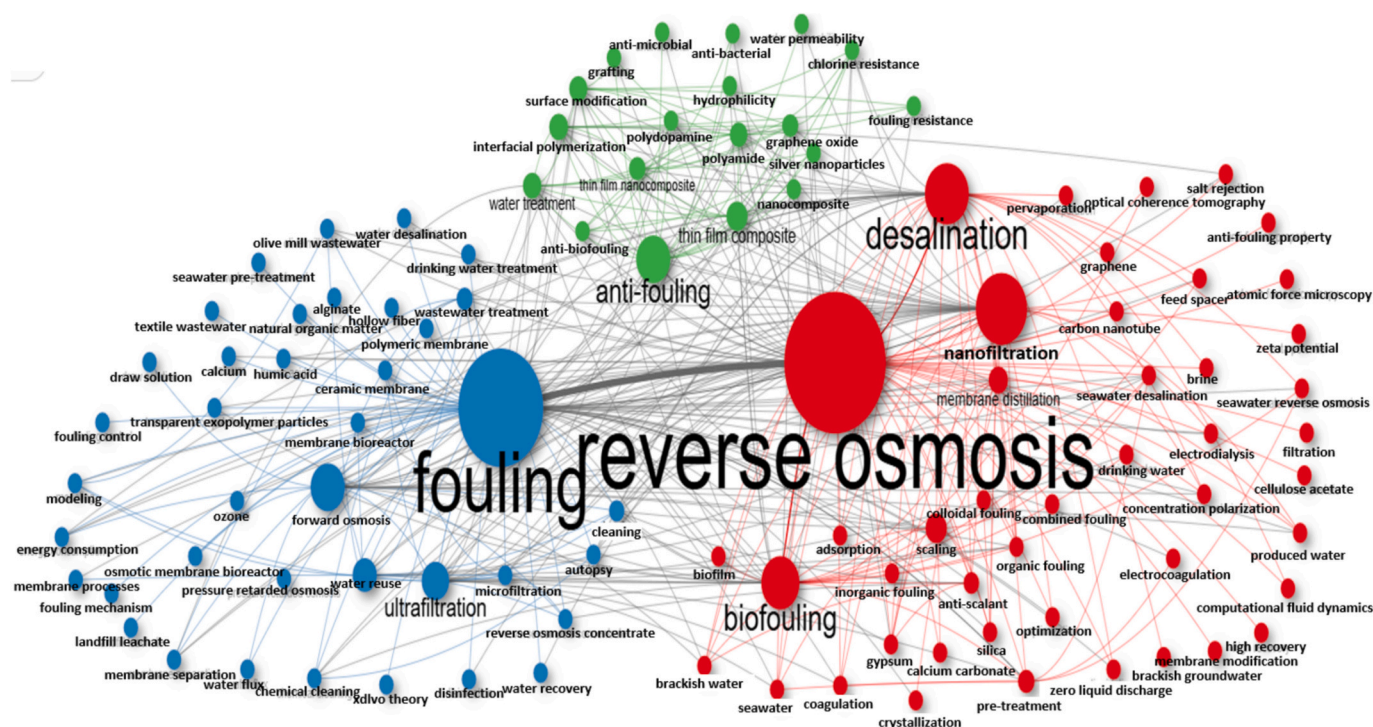


**Fig. 3.** Keywords co-occurrence analysis of research conducted in the field of RO membrane fouling during the past 10 years.

= 262) and it reveals that ‘thin film composite’ (F = 128), and ‘interfacial polymerization’ (F = 106) are commonly linked to the topic of anti-fouling. In addition to ‘interfacial polymerization’, the most frequently investigated membrane modification technique is ‘surface modification’ (F = 101).

Moreover, the term ‘thin film nanocomposite’ with an occurrence of 85, and high values of centrality parameters shows the inclination of researchers towards nanocomposites to develop fouling-resistant membranes. Among the nanomaterials used, our analysis shows that ‘graphene’, ‘carbon nanotubes’ (red cluster), ‘graphene oxide’, and ‘silver nanoparticles’ (green cluster) are the most commonly studied nanoparticles. These nanoparticles and their antifouling performances are also discussed in the following sections. It is interesting to note that the hydrophilicity (green cluster), and zeta potential (red cluster) are the only two membrane surface properties that have been studied in detail showing their significance in membrane fouling. These properties are discussed in detail in [Section 3.1](#). The ‘polyamide’, ‘polydopamine’ (green cluster), and ‘cellulose acetate’ (red cluster) is the most investigated membrane materials. It is also worth noting that the ‘polymeric membrane’ and ‘ceramic membrane’ (blue cluster) are the most common types of membrane studied in RO membrane fouling.

### 3. Membrane-foulant interactions

### 3.1. Influence of membrane properties on membrane–foulant interactions

To target and control fouling prevalence on RO membranes, it is important to understand and analyze the mechanism of foulant-membrane interaction and foulant-foulant interactions. Membrane fouling is a complex phenomenon that depends on a wide range of factors, including hydrodynamic operating parameters, characteristics of the feed water and foulant, and membrane properties (Fig. 4). Membrane properties refer to the characteristics of a membrane that influence its performance and functionality in different applications including surface charge, hydrophilicity/hydrophobicity, material composition, roughness, pore size, and surface functional groups [18].

### 3.1.1. Membrane surface charge

The interaction and mechanism between foulant colloids play a significant role in forming foulant on the membrane surface. If the foulant particles have opposite charges, attractive electrostatic forces can lead to agglomeration of the particles. A similar approach occurs whether the foulant particle has opposite charges to the membrane surface or charges that are identical to the membrane surface. Thereby, membrane-surface charge interactions can limit fouling by maintaining the membrane and foulant particles at similar charges to ensure repulsive force and reduce the interaction between them. The accumulation rate on the membrane surface is influenced by the relationship between particle collision and attachment coefficient. If foulant particles frequently collide with the membrane surface coupled with a large attachment coefficient, more particles will adhere, leading to faster accumulation and the formation of larger aggregates [19]. In high ionic strength solutions such as seawater, the interactions between particles are primarily governed by acid-base interactions rather than the electrical double-layer interactions, which become negligible in such conditions. While van der Waals forces, which include London dispersion forces and dipole-dipole interactions, are always present between particles, they alone cannot account for the significant shifts in pH and solution concentration observed in high ionic strength environments.

### 3.1.2. Membrane surface hydrophilicity/hydrophobicity

The wettability of a membrane is usually determined by the water contact angle,  $\theta$ . The larger the value between the membrane surface and the water droplet, the greater the hydrophobicity of the membrane surface [20]. The difference in the wettability of membranes helps in determining the suitable application field for each membrane. Hydrophilic membranes are widely used in water filtration processes as they exhibit improved water flow and reduced fouling on the membrane surface. Hydrophilic membranes possess specific functional groups, such as hydroxyl ( $-\text{OH}$ ), amine ( $-\text{NH}_2$ ), or carboxyl ( $-\text{COOH}$ ) groups, which can interact with water molecules through hydrogen bonding. The presence of these active functional groups enhances the affinity of hydrophilic membranes for water, making them more prone to wetting and promoting water permeation through the membrane structure.

**Table 1**

Frequency distribution table of most commonly used keywords, along with centrality parameters based on the network diagram in Fig. 3.

#	Keyword	Frequency	Main theme (as per Fig. 3)	Centrality parameters		
				Betweenness	Closeness	PageRank
1	Reverse osmosis	955	Reverse osmosis	3002.099	0.007	0.152
2	Nanofiltration	431	Reverse osmosis	487.161	0.006	0.056
3	Desalination	322	Reverse osmosis	428.320	0.006	0.055
4	Biofouling	311	Reverse osmosis	245.781	0.005	0.038
5	Scaling	125	Reverse osmosis	8.071	0.005	0.018
6	Membrane distillation	124	Reverse osmosis	9.443	0.005	0.013
7	Pre-treatment	82	Reverse osmosis	4.917	0.005	0.012
8	Anti-scalant	81	Reverse osmosis	3.821	0.005	0.011
9	Organic fouling	76	Reverse osmosis	0.009	0.004	0.006
10	Seawater desalination	62	Reverse osmosis	0.043	0.005	0.007
11	Brackish water	61	Reverse osmosis	0.106	0.005	0.008
12	Concentration polarization	44	Reverse osmosis	0.582	0.005	0.005
13	Seawater	41	Reverse osmosis	0.016	0.005	0.006
14	Gypsum	40	Reverse osmosis	0.105	0.004	0.005
15	Coagulation	32	Reverse osmosis	0.016	0.005	0.005
16	Fouling	740	Fouling	2191.565	0.007	0.12
17	Forward osmosis	263	Fouling	188.059	0.005	0.034
18	Ultrafiltration	197	Fouling	112.27	0.005	0.025
19	Water reuse	151	Fouling	23.196	0.005	0.024
20	Wastewater treatment	89	Fouling	0.783	0.005	0.009
21	Cleaning	78	Fouling	0.158	0.005	0.011
22	Microfiltration	57	Fouling	2.047	0.005	0.007
23	Membrane separation	47	Fouling	0.023	0.004	0.004
24	Chemical cleaning	39	Fouling	0.030	0.005	0.005
25	Autopsy	25	Fouling	0.039	0.005	0.006
26	Reverse osmosis concentrate	31	Fouling	0.051	0.004	0.003
27	Ceramic membrane	31	Fouling	0.015	0.004	0.003
28	Modeling	17	Fouling	0.026	0.004	0.004
29	Olive mill wastewater	16	Fouling	0.073	0.004	0.005
30	Anti-fouling	262	Anti-fouling	122.287	0.005	0.034
31	Thin film composite	128	Anti-fouling	2.260	0.005	0.017
32	Interfacial polymerization	106	Anti-fouling	3.943	0.005	0.015
33	Water treatment	102	Anti-fouling	1.733	0.005	0.013
34	Surface modification	101	Anti-fouling	5.827	0.005	0.014
35	Polyamide	97	Anti-fouling	4.533	0.005	0.014
36	Thin film nanocomposite	85	Anti-fouling	2.504	0.004	0.012
37	Graphene oxide	76	Anti-fouling	1.416	0.005	0.012
38	Anti-biofouling	58	Anti-fouling	0.717	0.004	0.005
39	Chlorine resistance	40	Anti-fouling	0.011	0.004	0.006
40	Fouling resistance	37	Anti-fouling	0.033	0.004	0.004
41	Polydopamine	34	Anti-fouling	1.608	0.005	0.005
42	Silver nanoparticles	27	Anti-fouling	0.121	0.004	0.004

Additionally, hydrophilic membranes can repel charged foulants through electrostatic repulsion, further improving their performance. This characteristic is advantageous in water filtration processes, as it enhances better water flow and minimizes fouling on the membrane surface. This promotes permeation and reduces the deposition of organic and particulate matter on the membrane surface. However, in some instances, when hydrophilic membranes interact with hydrophilic foulants, such as proteins or polysaccharides, they may still experience fouling due to adsorption or pore blocking. This suggests that hydrophilic membranes are not entirely immune to fouling, but the extent depends on the nature of the foulants present.

Hydrophobic membranes, in contrast to hydrophilic membranes, have surfaces that are predominantly composed of non-polar or low-polar materials. They typically exhibit a low affinity for water and a tendency to repel or resist wetting by water. The absence of active functional groups that can form hydrogen bonds with water leads to reduced interactions between the membrane surface and water molecules. Consequently, when hydrophobic membranes are used in aqueous environments, they are more prone to fouling by hydrophobic substances, such as oils and organic compounds, which adhere strongly to the membrane surface due to hydrophobic interactions. This can lead to significant pore blocking and reduced membrane efficiency. While hydrophobic membranes excel in separating non-polar compounds, their fouling resistance in aqueous applications is generally lower compared to hydrophilic membranes unless modified with hydrophilic coatings

[21].

The choice of membrane hydrophilicity or hydrophobicity should thus be carefully aligned with the intended application and the types of foulants expected. Hydrophilic modifications, such as the incorporation of zwitterionic polymers or hydrophilic polymers into hydrophobic membranes, have been shown to improve water flux and minimize fouling by reducing pore blocking and enhancing resistance to foulant adhesion [22,23]. In contrast, hydrophobic membranes offer superior performance in non-polar separation applications due to their selective affinity for non-polar molecules and resistance to organic fouling [24,25].

### 3.1.3. Membrane surface functional groups

Numerous studies have explored the influence of surface functional groups on fouling and scaling propensity in RO membranes in desalination processes. In their study, Liu et al. aimed to improve the permeability and anti-fouling properties of the RO membrane by modifying its surface with L-lysine, which contains functional groups such as amino and carboxyl groups. This modification significantly increased the membrane's surface hydrophilicity, enhancing its affinity for water molecules. As a result, the modified membrane demonstrated improved water permeability and higher water flux, with a 22.45 % increase in water flux compared to that of the unmodified membrane. Additionally, the salt rejection of the modified membrane increased to 98.53 % from the initial value of 95.44 %. Khoo et al. [26], successfully

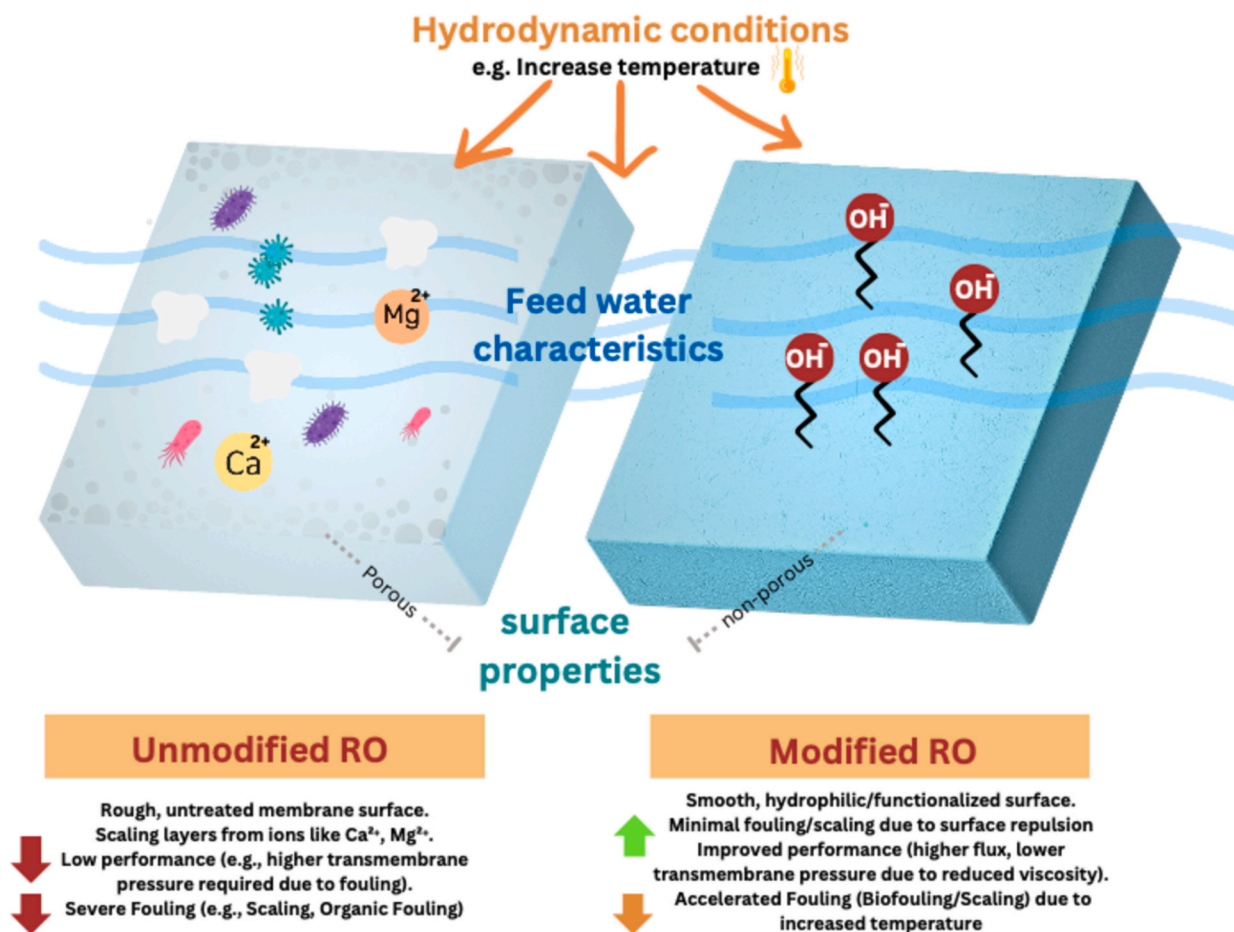


Fig. 4. Impact of hydrodynamic conditions, feed water characteristics, and surface properties on fouling interactions in functionalized versus non-functionalized RO membranes.

functionalized the RO membrane by depositing titania nanotubes onto its surface and subsequently coating it with polyacrylic acid. The study found that the acrylic acid-coated TFN membrane (AA-TFN) showed exceptional resistance to silica scaling at high silica concentrations. In comparison to the uncoated TFN and conventional TFC membranes, the AA-TFN membrane exhibited a significantly higher flux recovery rate (FRR) of 88 %. This improved performance was attributed to the enhanced surface hydrophilicity (with a contact angle of  $26^\circ$ ) and enhanced surface charge (with a zeta potential of  $-47$  mV) resulting from the deposition of the hydrophilic coating layer. These modifications effectively hindered the deposition of scales on the RO membrane surface.

#### 3.1.4. Membrane pore size and distribution

The size of membrane pores plays a crucial role in the occurrence of reversible and irreversible fouling, as highlighted by Sano et al. [28]. Fouling typically accumulates either on the external membrane surface, forming a cake layer, or within the membrane pores, causing pore blockage. Pore-blocking fouling occurs when foulants accumulate and partially or completely obstruct the membrane pores. The significance of membrane pore size concerning fouling is primarily based on size exclusion. The pore size determines whether foulants can pass through the membrane or become trapped on its surface [29]. It is well known that membrane pores have a direct impact on fouling. If the pore size is larger than the foulant particles, the foulants can easily traverse the membrane, leading to fouling. This presence of foulants reduces the available space for water molecules to pass through, resulting in decreased water permeability and increased salt passage [187].

Conversely, if the pore size is smaller than the foulant particles, fouling can be minimized, as the foulants are more likely to be rejected and unable to penetrate the membrane. A uniform distribution of pores across the membrane surface is essential for consistent filtration and reduced risk of localized fouling. Chow & Karnik [30], investigated the influence of pore size distribution of nano-porous atomically thin RO membranes on fouling propensity and overall desalination efficiency. They found that the membranes with a narrow and uniform pore size distribution exhibited reduced fouling tendencies by promoting an even flow of water and ions, preventing the accumulation of foulants and thick fouling layers. In contrast, the membranes with a wide pore size distribution had a higher fouling propensity due to the ingress of larger molecules, resulting in thicker fouling layers, reduced salt rejection, and decreased water permeability, which negatively impacted desalination efficiency.

In general, RO membranes with smaller pore sizes proved to be more resistant to fouling because they effectively reject larger foulants. For example, Corcos et al. [31] noted that decreasing the pore size of covalent organic frameworks (COFs) in TFC membranes improved solute rejection by inhibiting the passage and accumulation of foulants. Similarly, Zhao et al. reported that membranes with smaller pore sizes exhibited reduced fouling tendencies due to the limited passage and accumulation of algae cells and organic matter.

#### 3.1.5. Membrane surface roughness

RO membrane surface roughness influences fouling behavior by impacting foulant adhesion. Rough surfaces provide more attachment sites for fouling, making them more susceptible to fouling, while

smoother surfaces have fewer sites for fouling attachment and are easier to clean. In their study, Hobbs et al. [34] observed that RO and nano-filtration (NF) membrane surface roughness played a significant role in fouling behavior. They found that the presence of roughness on the membrane surface created crevices, defects, and irregularities, which in turn facilitated the adhesion of foulants. These foulants tended to accumulate in the recesses and irregularities of the rough surface, forming cake layers that reduced the effective membrane area available for filtration. As a result, permeate flux decreased and pressure drop across the membrane increased, ultimately leading to a negative impact on overall filtration performance. Furthermore, Yin et al. [35] revealed that there is a significant correlation between RO membranes' surface roughness and fouling. They observed that membranes with rougher surfaces tended to experience higher fouling rates compared to smoother membranes. Also, the roughest surface membrane exhibited the most significant flux decline. Vatanpour et al. [36] found that the incorporation of amine-functionalized MWCNTs into PES membranes resulted in a significant reduction in fouling. The membrane functionalization from the presence of MWCNTs created a smoother surface with modified surface properties of the membrane, which hindered foulant adhesion and reduced fouling propensity. The improved fouling resistance was attributed to the repulsive interactions between the functional groups on the MWCNTs and the foulants, preventing their attachment to the membrane surface.

Membranes with rougher surfaces enable fouling deposits to penetrate into surface irregularities, making their removal challenging during conventional cleaning methods. This reduces cleaning efficiency and increases the risk of persistent fouling which is difficult to remove completely [37]. Porosity can also lead to the entrapment and retention of foulants within the membrane matrix, resulting in the formation of fouling layers inside the membrane. Such trapped foulants are challenging to remove through regular cleaning methods, exacerbating fouling issues. Baig et al. [32] synthesized a RO membrane with enhanced properties, transitioning it from hydrophobic to highly hydrophilic, and significantly reducing surface roughness (Table 2). Moreover, their coated membranes exhibited exceptional anti-biofouling properties, as depicted in Fig. 5(a). In contrast to the unmodified membrane, which displayed larger colonies and thick biomass in various regions, the modified membrane surface had a notably different profile, indicative of its anti-biofouling mechanism (Fig. 5b).

### 3.1.6. Membrane material composition

Membrane material composition has different affinities for different types of foulants. There is a relationship between the chemical composition of the membrane and the strength with which foulants adhere to the membrane surface. Commonly used membranes can be classified according to the material of synthesis, and they are categorized into ceramic membranes, metal membranes, and organic (polymeric) membranes. Among them, organic membranes are the most frequently used in desalination as they are less expensive and flexible [47]. They do have limitations, though, including a short lifespan, easily prone to foul, and poor performance at high pressures and temperatures. Nonporous polymeric materials are utilized to create organic membranes; among the most popular ones are cellulose acetate, polyvinylidene fluoride, polyethylene, and polysulfone [48].

Conversely to organic membranes, ceramic and metallic composite membranes have defined pore structures and are very chemically and thermally resistant, but they are also brittle, inflexible, and very costly. Ceramic membranes are theoretically hydrophilic since they exhibit hydroxyl groups on the membrane surface which facilitate in hindering the attachment of foulant particles [49]. In general, polyamide TFC membranes and cellulose acetate RO membranes exhibit a degree of negative surface charge and hydrophilicity and thus would naturally repel foulant accumulation on the membrane surface [50].

A consensus can be derived from the comprehensive analysis (Table 2) and comparison of various studies on membrane-fouling

interactions. It is evident that enhancing membrane properties through strategic functionalization is a pivotal strategy for addressing fouling challenges in membrane processes. As shown in Table 2 and Fig. 4, modifying membrane surfaces has the potential to improve fouling resistance, anti-scaling behavior, and overall performance. It is evident from these findings that tailored membrane functionalization plays an important role in advancing the effectiveness and sustainability of membrane-based technologies. Future research and development in this direction will prove crucial to overcoming fouling interactions and ensuring the continued success of membrane processes. Based on the findings from Table 2, there are multiple factors that dominate the enhancement antifouling RO membrane properties which are a combination of Increased hydrophilicity, decreased surface roughness, regulated surface charge, and the addition of antibacterial agents or nanomaterials that support photocatalytic and electrostatic repulsion properties. The combination of these mechanisms can decrease biofouling, and increase the overall durability and functionality of RO membranes in water treatment.

### 3.2. Influence of hydrodynamic conditions on membrane-foulant interactions

Membrane fouling is a common challenge in RO membrane-based separation processes, and various operational parameters can influence its occurrence and severity such as permeation flux, cross-flow velocity, transmembrane pressure, and module and spacer design. Cross-flow velocity refers to the velocity of the liquid flowing tangentially across the membrane surface. Adequate cross-flow velocity enhances shear forces, preventing fouling by disrupting the accumulation of particles and organic matter on the membrane. It is commonly understood that increasing cross-flow velocity generally leads to higher permeate flux, as it enhances shear forces and reduces the accumulation of solutes and particles on the membrane surface. This is possible because higher cross-flow velocities have a beneficial impact on both the mass transfer coefficient of the solute and the level of mixing near the RO membrane surface [51]. The enhanced mixing associated with larger cross-flow velocities helps reduce the aggregation of feed solids in the gel layer. This reduction occurs due to the increased diffusion of these components back into the bulk solution, effectively mitigating the effects of concentration polarization (CP). The degree of concentration polarization is related to the ratio of water flux ( $J$ ) to the boundary layer mass transfer coefficient ( $k$ ). Water flux represents the rate at which water permeates through the membrane, while the boundary layer mass transfer coefficient represents the efficiency of mass transfer between the feed solution and the membrane surface. As a result, membrane fouling is commonly recognized as a phenomenon driven by flux, which is intricately tied to the transmembrane pressure [10].

However, excessively high cross-flow velocities can also have negative effects. Very high velocities may cause turbulence, resulting in increased pressure drop, energy consumption, and potential membrane damage. Zhao et al. [10] revealed that this behavior can be attributed to the higher pressure drop resulting from an increased rate of corrosion associated with the higher flow rate. As a result, the permeate flow rate decreases, leading to an overall increase in specific energy consumption in the RO system. Therefore, there is an optimal range of cross-flow velocities for maximizing permeate flux without compromising system performance and membrane integrity. Optimal cross-flow velocity promotes the continuous sweeping of foulants away from the membrane surface, reducing their deposition.

On the other hand, temperature has a significant impact on RO membrane performance, especially regarding fouling. Shigidi et al. [52] observed that raising the temperature from 5 to 55 °C led to a remarkable increase in permeate flux, exceeding 100 %. This increase in flux can be attributed to changes in the physical properties of the membrane surface, such as pore size swelling and water diffusion through the membrane. These changes enable a higher number of ions to pass

**Table 2**

Comparative Analysis of functionalized RO Membranes: Evaluating material properties and their influences on fouling in water desalination.

Membrane/ experimental setup	Membrane performance before functionalization	Membrane modification	Antifouling performance	Fouling mechanism	Fouling resistance mechanism	Summary	References
Membrane functionalization: Aminated Graphene Oxide and Polydopamine Nanospheres Plugging Feed: 2000 ppm NaCl + 890 $\mu\text{g L}^{-1}$ NDMA (contaminant)	Rejection rate: 69.2 $\pm$ 2.1 % Permeate flux: 11 LMH Pressure: 12 bars	Hydrophilic ( $\text{NH}_2$ & OH) groups; Neutral surface charge; High porosity; Surface roughness ( $S_q$ ) 59.5 nm	Nature of fouling: Organic fouling (NDMA) Rejection rate: 89.3 $\pm$ 2.7 %	Adsorption	(a) Suppression of Carboxyl Groups, (b) Reduced Surface Roughness, (c) Enhanced Hydrophilicity, and (d) Bactericidal Properties	Increased cross-flow velocity could reduce particle deposition and organic fouling in large- scale applications. Surface roughness plays a critical role in mitigating fouling; the reduction in roughness after modification enhances performance in desalination plants. Upgrading pumps or optimizing membrane module designs could facilitate increased crossflow velocity in practice.	[38]
Membrane functionalization: polyglycidol decorated hyperbranched copolymer commercial Feed: 2000 ppm NaCl solution + $\sim 10^6$ /ml <i>P. aeruginosa</i>	Rejection rate: 94 % Permeate flux: 28.6 LMH Pressure: 15 bars	Hydrophilic ( $\text{NH}_2$ & OH) groups; Positive surface charge; Surface roughness ( $S_q$ ) 21.6 nm	Nature of fouling: Biofouling ( <i>P. aeruginosa</i> ) Inhibition rate: High ( $\approx 70$ %) Flux recovery ratio (FRR): 95 %	Adsorption	(a) Increased Hydrophilicity, (b) Reduced Roughness, (c) Mostly positive surface charge, (d) Reduced Bacterial Adhesion	Practical desalination applications should focus on membrane surface charge. Positively charged surfaces demonstrate excellent biofouling resistance, but surface smoothness is equally important in enhancing antifouling efficiency. Cleaning protocols with backwashing or chemical cleaning are essential for maintaining membrane performance over time.	[32]
Membrane functionalization: Zwitterion functionalized graphene oxide/PA- TFN Feed: 1000 ppm NaCl + 200 ppm BSA solution	Rejection rate: 95.3 % Permeate flux: 35 LMH Pressure: 15 bars	Hydrophilic (sulfonic acid and ammonium) groups; Neutral surface charge; Surface roughness ( $S_q$ ) 13.1 nm	Nature of fouling: Organic fouling (Proteins) Fouling resistance: High Flux recovery ratio (FRR): 94 %	Adsorption	(a) Increased hydrophilicity, (b) Reduced surface roughness	Zwitterionic functional groups provide strong anti- protein fouling properties, making these membranes ideal for reuse. Automated cross-flow velocity control systems can enhance long- term performance in desalination plants. Additionally, optimizing surface hydrophilicity through chemical modification can improve flux recovery in repeated cycles.	[39]
Membrane functionalization: Oxidized multiwalled carbon nanotubes (MWCNTs) into PA- TFN Feed: 2000 ppm NaCl + 500 ppm BSA solution	Rejection rate: 96.1 % Permeate flux: 20.3 LMH Pressure: 15 bars	Hydrophilic (OH & COOH) groups; Dense, finely dispersed grainy structure (reduced surface roughness)	Nature of fouling: Organic fouling (Proteins) Fouling resistance: High Fouling flux: $\approx 27\text{--}25 \text{ kg/m}^2 \text{ h}$	Adsorption	(a) Increased hydrophilicity, (b) Reduced surface roughness, (c) hydrogen bonds	Reduced surface roughness from MWCNT incorporation prevents pore clogging, though agglomeration must be managed. Regular physical cleaning, such as backwashing, combined with low-intensity chemical cleaning, can sustain membrane performance. Implementing automated cross-flow velocity control can further minimize fouling by ensuring consistent flow and shear forces at the membrane surface.	[40]
Membrane functionalization: Graphitic carbon nitride (COOH-g- $\text{C}_3\text{N}_4$ ) nanosheets in	Rejection rate: 96.02 % Permeate flux: 59.37 LMH	Hydrophilic (COOH); Negative surface charge; Surface	Nature of fouling: Organic fouling (Proteins) BSA flux: 60 L/ $\text{m}^2 \text{ h}$	Adsorption	(a) Increased hydrophilicity, (b) Negative surface charge, (c) Reduced surface	Negative surface charge contributes to excellent fouling resistance due to electrostatic repulsion, leading to a high rejection	[41]

(continued on next page)

Table 2 (continued)

Membrane/ experimental setup	Membrane performance before functionalization	Membrane modification	Antifouling performance	Fouling mechanism	Fouling resistance mechanism	Summary	References
PA-TFC Feed: 2000 ppm NaCl + 100 ppm BSA		roughness ( $S_q$ ) 4.1 nm	Rejection rate: 98.1 %		roughness, (d) Repulsion effect.	rate of 98.1 %. These membranes demonstrate strong potential for implementation in high- salinity environments.	
Membrane functionalization: Nanocomposite photocatalyst of titanium dioxide/ carbon dots (0.02 TiO <sub>2</sub> /CDs) into PA Feed: 100 ppm solution of Humic acid (HA)	Rejection rate: 96.1 % Permeate flux: 40.5 LMH Pressure: 15 bar Flux recovery ratio (FRR): 94.4 %	Hydrophilic (COOH, OH, & CO) groups; Negative surface charge; Surface roughness ( $S_q$ ) 14.1 nm	Nature of fouling: Organic fouling (HA) Flux recovery ratio (FRR): 98 % under UV exposure Total fouling ratio (RT): $\approx$ 7 %	Adsorption	(a) Electrostatic repulsion, (b) surface smoothness, (c) hydrophilicity, (d) Photocatalytic Activity	Photocatalytic degradation of humic acid under UV light positions this membrane as a strong candidate for desalination plants facing organic fouling challenges. Photocatalytic regeneration offers a low- energy, sustainable antifouling solution. Incorporating UV reactors into desalination facilities can further enhance membrane performance and mitigate fouling.	[42,43]
Membrane functionalization: Carboxyl group- functionalized carbon nanospheres (CNS- COOH) and silver- coated in PA-TFN Feed: 2000 ppm NaCl +5 ppm solution of Humic acid (HA)/ 200 $\mu$ L of <i>E. coli</i>		Hydrophilic (COOH); Negative surface charge; Surface roughness ( $S_q$ ) 59.4 nm	Nature of fouling: Organic fouling (HA) & biofouling ( <i>E. coli</i> ) Flux recovery ratio (FRR): High Rejection rate: 96.7 % HA flux: 56.4 L/ m <sup>2</sup> -h Antibacterial efficiency: 93.5 %	Adsorption	(a) Increased hydrophilicity, (b) surface smoothness, (c) Carboxyl groups caused oxidative stress reaction (inhibition of bacterial growth), (d) Ag NPs disrupted bacterial proteins via affinity for thiol groups	Silver nanoparticles offer strong biofouling resistance, essential for desalination plants facing microbial contamination. To maintain antibacterial properties, practical integration may include periodic silver ion regeneration or surface functionalization. In areas with high biofouling risks, silver-coated membranes serve as a sustainable long- term solution.	[44]
Membrane functionalization: Fe <sub>2</sub> O <sub>3</sub> /TS-1 NPs in TFN Feed: 2000 ppm NaCl + 200 ppm BSA	Rejection rate: 94.99 % Permeate flux: 40.5 LMH Pressure: 15 bar	Hydrophilic (OH); Negative surface charge; Surface roughness ( $S_q$ ) 22.44 nm	Nature of fouling: Organic fouling (Proteins) Flux recovery ratio (FRR): 95 %	Adsorption	(a) Surface smoothness, (b) Negative surface charge, (c) enhanced hydrophilicity	The antifouling performance is significantly enhanced by hydrophilicity and surface smoothness. Plants can implement real-time monitoring of surface charge and surface roughness to maintain the efficiency of the membranes in prolonged operations.	[45]
Membrane functionalization: Cellulose Nanofibers- Hybridized Ti <sub>3</sub> C <sub>2</sub> T <sub>x</sub> PA Feed: 2000 ppm NaCl + 200 ppm BSA/HA	Rejection rate: 98.5 % Permeate flux: 26.7 LMH Pressure: 16 bar	Hydrophilic (OH); Negative surface charge	Nature of fouling: Organic fouling (Proteins) & Flux recovery ratio (FRR): 81.6 %	Adsorption	(a) Surface smoothness, (b) formation of hydration layer on membrane surface, (c) strong electrostatic repulsion	To further optimize performance in desalination plants, increasing cross-flow velocity can minimize fouling by enhancing shear forces at the membrane surface. Practical methods include adjusting flow rates or utilizing turbulent flow promoters, such as spacers or vortex generators, to maintain membrane efficiency over extended operations.	[46]

through the membrane, leading to reduced removal process efficiency and potential fouling issues. Additionally, it is important to note that elevated temperatures can create favorable conditions for bacterial colonization and biofilm development, potentially exacerbating biofouling [53]. Moreover, studies demonstrated that higher temperatures contributed to an escalation in RO membrane scaling [54,55]. This was evident through a substantial reduction in flux over time,

accompanied by an increase in the mass of precipitated crystals and the thickness of the scale layer. Hence, the impact of temperature on membrane performance should be carefully considered to mitigate fouling and scaling as well as maintain optimal system efficiency.

Transmembrane pressure (TMP) is another hydrodynamic fouling factor that can affect RO membrane processes. TMP is the pressure difference across the membrane, and it can affect the driving force for

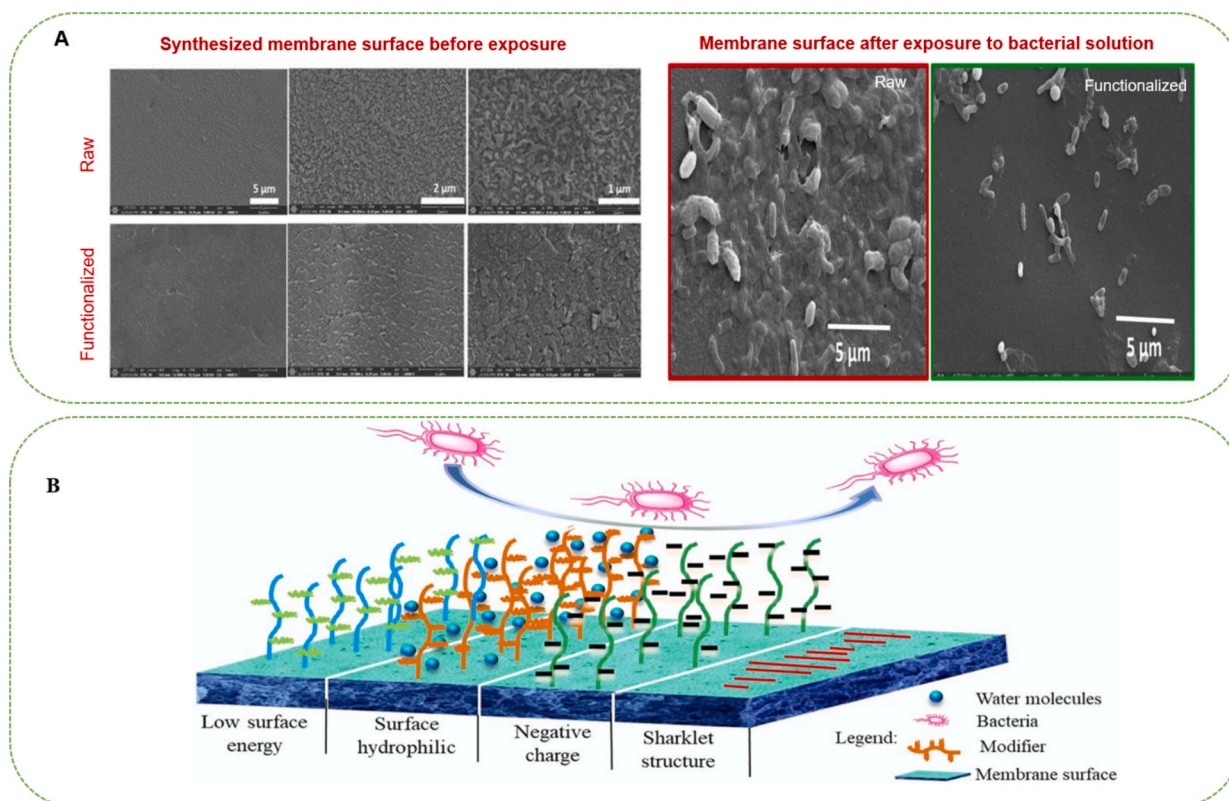


Fig. 5. (a) Influence of RO surface functionalization with antiadhesion and antibacterial properties on resisting biofouling [32]. (b) Schematic diagram of anti-fouling RO membrane mechanism [33].

filtration and can influence fouling. Elevating the TMP can lead to greater accumulation and deposition of fouling agents on the membrane surface. Consequently, this leads to a decline in membrane performance, a decrease in water flux, and an escalation in pressure drop across the membrane. Zhou et al. [56] noted that the fouling mechanism in RO membranes varied depending on the TMP applied. At lower TMP values, reversible fouling dominated, where fouling agents could be more easily removed through cleaning procedures. In contrast, higher TMP levels result in irreversible fouling, making it more challenging to restore membrane performance.

### 3.3. Influence of feed solution/water composition on membrane-foulant interactions

The composition of the feed solution or water has a significant influence on the interactions between the membrane and foulants in RO membrane processes. The feed solution composition, including its chemical constituents, can significantly influence membrane fouling, which includes pH, ionic strength, and calcium concentration. The pH of the feed water affects the surface charge of the foulants and the membrane. Varying pH levels can change the charge distribution, resulting in altered electrostatic interactions between the foulants and the membrane surface. Specifically, low pH and high divalent cations tend to speed up the process of organic fouling. This occurs because the charge properties of organic matter decrease due to the neutralization of functional groups, as well as the formation of complexes between organic compounds and calcium ions. Elevated pH levels of feed water affect both the charge properties of bulk organic foulants and their interaction with membrane surfaces. Increasing pH leads to the development of dense fouling layers on the membrane surface, as organic foulants accumulate in multiple layers. Additionally, the electrostatic repulsion between organic foulants and the membrane surfaces decreases, resulting in an accelerated accumulation of foulants on the

membrane surface [57].

When it comes to desalinating seawater through RO, where the concentration of ions is high, alterations in pH have minimal impact on the decline of flux rate. That is because higher ionic strength in the feed solution has an impact on the electrostatic interactions between the foulants and the charged surface of the membrane. Specifically, higher ionic strength can enhance the screening effect, reducing the electrostatic forces between foulants and the membrane. Consequently, the pH of the feed water does not play a significant role in the occurrence of organic or biological fouling during seawater desalination using RO membranes [58]. However, in some cases, alterations in pH levels can significantly affect the removal of particulate and colloidal contaminants usually found in seawater. For instance, boron is one of the main constituents of seawater, and it poses a significant challenge in the removal process when it comes to seawater RO desalination. Increasing the pH of the feed water enhances boron ionization and rejection, but it can lead to salt precipitation and membrane scaling. Consequently, efficient boron removal often requires multiple RO stages with different pH values: the first stage focuses on salt removal at a lower pH, while the second stage targets boron removal at a higher pH [188]. Moreover, Pranić et al. [59] found that pH values had a significant impact on the desalination efficiency of multi-ionic solutions using RO. At lower pH values, the rejection of ions improved due to increased electrostatic repulsion between the membrane and ions. However, extremely low pH levels resulted in membrane damage and reduced performance. Higher pH values enhanced the rejection of divalent ions but also led to higher scaling potential of RO membranes.

The specific ions present in the feed water may have different affinity towards the membrane surface or foulants, leading to complexation or precipitation phenomena. For instance, calcium ions ( $\text{Ca}^{2+}$ ) can form insoluble salts or complexes with certain foulants, contributing to fouling. An increase in divalent cation concentration, particularly  $\text{Ca}^{2+}$ , enhances organic fouling. The presence of calcium ions results in the

neutralization of functional groups and the formation of organic-calcium complexes, diminishing the charge properties of organic matter and facilitating fouling of the membrane [191]. Additionally, increased calcium levels in feed water might increase the risk of gypsum scaling on the surface of the RO membrane. This occurs as calcium ions combine with sulfate ions to form gypsum crystals, which adhere to the membrane and result in scaling [54,55]. Calcium ions can also form complexes with alginate, altering its conformation and increasing its adhesion to the membrane surface. This results in more severe fouling and reduced membrane performance.

Additionally, the physicochemical properties of the foulants, such as their sizes, charges, structures, functional groups, and hydrophobicity, influence their interactions with the membrane. The composition of the feed solution affects these properties, which in turn affect the fouling behavior. For example, the presence of hydrophobic foulants or foulants with specific functional groups can enhance their attachment to hydrophobic regions of the membrane. Landsman et al. [60] found that hydrophobic NOM containing aromatic and carboxyl groups is promoted by divalent cations, such as calcium and magnesium, leading to fouling of the PA membrane. The hydrophobic nature of these foulants allows them to interact favorably with the hydrophobic regions of the membrane surface facilitating their attachment and subsequent fouling.

### 3.4. Practical solutions for desalination plants to enhance membrane performance

A strategic technique to reduce fouling and scaling in RO membranes and to enhance the performance of desalination plants is increasing cross-flow velocity. Various practical solutions such as the optimization of the configuration of spacer designs and tangential flow. This tactic leads to an increased shear force applied on the surface of the membrane which in turn causes enhanced prevention of foulant accumulation [62]. Moreover, concentration polarization can be reduced and permeate flux can be enhanced through the modification of transmembrane pressure as well as operating temperatures. These modifications and adjustments should be managed carefully to avoid any elevation in fouling problems [46].

Furthermore, modifications to the membrane surface, such as the application of hydrophilic coatings like polyacrylic acid or polydopamine, and the incorporation of nanomaterials such as titanium dioxide or graphene oxide, have demonstrated improvements in membrane hydrophilicity, permeability, and resistance to foulant deposition. The integration of hybrid organic-inorganic membranes, combined with optimized feed spacer geometries, further enhances fouling resistance and promotes uniform water flow. These combined approaches help sustain higher cross-flow velocities, ultimately improving desalination efficiency and lowering operational costs.

## 4. Strategies for RO membrane development to inhibit membrane fouling

### 4.1. Modification of the top PA layer of the RO membrane

To tackle the unavoidable fouling and scaling problems that arise in the top PA layer of TFC RO membranes, researchers have extensively explored various materials to modify and enhance the properties of the PA layer. Broadly, these materials can be classified into three categories: organic materials, inorganic materials, and hybrid materials composed either of organic/inorganic or organic/organic components.

#### 4.1.1. Organic materials

An effective approach to mitigate the tendency of surface fouling and scaling in RO membranes is the incorporation of hydrophilic polymers onto the PA selective layer [26]. Chen and Cohen [8], for instance, grafted surface-tethered polyacrylic acid (PAA) onto a commercial RO membrane (Toray BWRO) and reported that the resultant membrane

could significantly inhibit the deposition and growth of mineral crystals onto the membrane surface. PAA is an inherently hydrophilic material due to the abundance of carboxylic acid groups ( $-\text{COOH}$ ) along its polymer chain. The PAA-grafted RO membrane only suffered an 11 % flux decline throughout a 24-h performance testing using 2611 ppm of gypsum and was found to be able to attain a 100 % flux recovery rate after subjecting to a DI cleaning. Meanwhile, the unmodified TFC membrane recorded a flux decline and FRR of 16 % and 92 %, respectively. They postulated the higher flux recovery to the collapsed PAA chains configuration at high ionic strength of gypsum solution that swells during cleaning with DI water, helping the detachment of scale crystals.

Polyvinyl alcohol (PVA) has also been proven to be a versatile coating material for modifying the surface properties of RO membranes, alongside PAA. This is primarily due to its adhesive nature and neutral charge. Some commercially available RO membranes such as Hydranautics LFC3 and FilmTec BW30FR are functionalized with PVA to enhance their fouling resistance. Owing to the positive features of PVA, Hu et al. [63] covalently attached it to the TFC membrane via surface coating and reported that the surface-modified membrane demonstrated a significantly higher FRR (90.8 %) in comparison to the neat TFC membrane (79.2 %) after being subjected to the 40-h filtration of 200 ppm BSA solution, which mimics a common protein found in wastewater and surface waters. The authors attributed the improvement to the higher hydrophilicity and less negative charge of the PVA-coated TFC membrane that minimized the adsorptive interactions of organic foulant with the membrane surface. The increased membrane stability against organic fouling prompted the researchers to further compare the anti-fouling performance of the PVA-coated TFC membrane with the commercial BW30FR for the tertiary treatment of industrial effluent. As shown in Fig. 6(a), the PVA-coated TFC membrane exhibited comparable flux antifouling properties as the BW30FR, recording a flux decline of 21.4 % and FRR of 90.0 %, while the BW30FR recorded 20.5 % and 89.5 %, respectively.

Aiming to further improve the permeability of the PVA layer, Zhang et al. [67] synthesized sulfonated PVA (sPVA) via esterification of PVA using sulfuric acid and coated it onto the PA layer with the use of glutaraldehyde as a crosslinker. The fouling behavior of pristine, PVA-coated, and sPVA-coated TFC membranes was investigated for a filtration period of 12 h using an organic solution containing 2000 ppm cetyltrimethylammonium bromide (CTAB) and 2000 ppm NaCl. Compared with the flux of pristine TFC membrane which declined by 60.4 %, both PVA and sPVA-coated TFC membranes displayed relatively low flux decline, recording 46.4 % and 44.3 %, respectively. The fouling propensity of cationic CTAB typically relies on the surface charge of the membrane. Thus, the introduction of neutrally charged PVA molecules to TFC membranes could reduce their electronegativity, which, in turn, inhibits the adhesion of foulants to the membrane surface. It must be noted that the presence of hydrophilic sulfonic acid groups on the sPVA coating film further enhanced the membrane antifouling property.

Another hydrophilic polymeric material that showed promising impacts in improving the membrane fouling resistance is chitosan. Its popularity as a functionalization material is attributed to its eco-friendly nature as it is derived from chitin, which contains an abundance of amino and hydroxyl groups. In 2018, Mehta et al. grafted the natural biopolymer onto a commercial RO membrane (Hydranautics CPA2) and reported that under optimum grafting conditions, the resultant membrane demonstrated huge improvement in surface hydrophilicity, with a contact angle measuring  $29.87^\circ$  versus  $46.37^\circ$  of the pristine TFC membrane. This in turn helped promote the membrane performance stability during the BSA filtration process (5000 ppm), where the chitosan-grafted TFC membrane recorded a permeate flux decline of 42.30 % in comparison to 49.20 % of the pristine TFC membrane after 4 h of filtration.

Polydopamine (PDA), owing to its abundant catechol groups, has previously been employed to coat the surface of the PA layer [68]. This

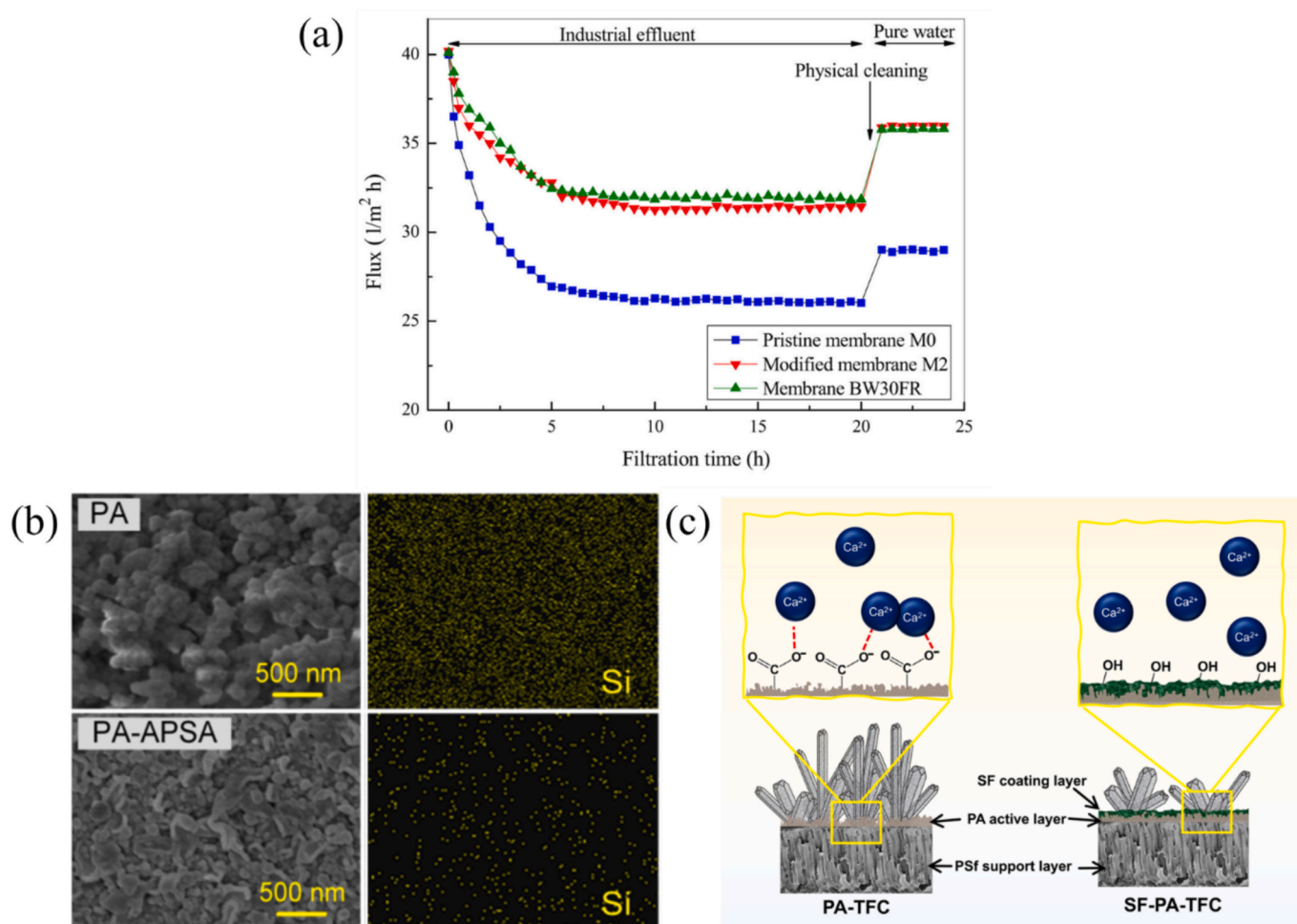


**Fig. 6.** (a) Time-dependent flux of neat TFC, PAA-modified TFC and commercial BW30FR membranes in the filtration of industrial effluent [63], (b) SEM images and EDX spectra of pristine (top) and APSA-modified (bottom) TFC membranes after combined silica scaling and HA fouling experiment followed by a simple physical cleaning [64] and, (c) Schematic illustration showing the mechanism underlying the anti-scaling effect of the silk fibroin (SF)-modified TFC membranes [66].

coating serves the purpose of preventing the attachment of organic foulants to the membrane surface. In a study conducted by Zhao et al. [69], the researchers observed an enhancement in fouling resistance for the RO membrane after applying a PDA coating. During a 24-h filtration of a 100-ppm sodium alginate (NaAlg) solution, the flux decline of the RO membrane improved from 18 % to 11 % following the PDA coating. Nevertheless, it must be pointed out that the conventional self-polymerization process of dopamine often requires a long reaction time (up to 6 h). To address this issue, Wang et al. [72] introduced a strong oxidant - sodium periodate ( $\text{NaIO}_3$ ) into a dopamine solution. This modification successfully reduced the coating duration for the RO membrane to 20 min. The resultant PDA-coated membrane was reported to exhibit 36 % higher flux than the pristine membrane when tested against soybean oil-in-water emulsions (1 w/v%) for 12 h.

Separately, Guan et al. [73] and Hao et al. [64] utilized sulfonic groups to customize the dual functionality of TFC membranes to simultaneously impart antifouling and anti-scaling properties. Guan et al. [73] covalently bonded hydroxylamide-O-sulfonic acid (HOSA) to the native carboxylic groups of the PA layer via carbodiimide-mediated reaction. This approach reduced the interaction of silica species with the sulfonic groups and led to slower nucleation of silica on the membrane surface. The results showed that the membrane functionalized with sulfonic groups exhibited a reduced propensity for scaling in comparison to the control membrane. This was demonstrated during a 20-h run with a silica solution, where the flux decline decreased from 22 % to 5 %. A simple rinsing with DI water allowed the sulfonic-modified TFC

membrane to recover up to 92.5 % of its initial water flux compared to 85 % as shown by the pristine membrane. When testing the membranes with a scaling experiment using 340 mg/L  $\text{Na}_2\text{SiO}_3$  for 24 h, Hao et al. [64] also observed a remarkable improvement in flux decline rate (from 72 % to 10 %) in the resultant membrane after grafting 3-amino-1-propanesulfonic acid (APSA) onto the PA layer. These findings strongly indicated that the presence of sulfonic groups has a beneficial impact in reducing membrane scaling.

In addition, Guan et al. [73] and Hao et al. [64] reported that the resultant membranes experienced significant enhancement in fouling reversibility with the presence of sulfonic groups in the PA layer. After the filtration of NaAlg, the HOSA-modified TFC membrane was able to recover 88.4 % of its initial water flux, while the unmodified recovered only 75 % [73]. Following the improvement in individual scaling and fouling resistance, further investigation was conducted to assess membrane behavior in a combined scaling and organic environment. In a mixed feed solution consisting of silica and alginate, the HOSA-modified TFC membrane recorded higher FRR (80 %) relative to the control TFC membrane (70 %). Comparing the results from the individual and combined scaling/fouling tests, Guan et al. [73] observed no significant difference in the synergistic effects of combined alginate-silica, noting that the presence of organic matter has negligible effects on silica interaction with the membrane surface. The same observation was reported by Hao et al. [64], where the APSA-modified TFC membrane recovered ~62 % of the initial water flux as opposed to ~50 % by the pristine TFC membrane after 24-h filtration of combined HA and silica.

As can be seen in Fig. 6(b), in contrast to the pristine TFC membrane surface that was entirely covered with foulants, the ridge-and-valley structure of the APSA-modified membrane was still visible, indicating that the modified membrane had a better fouling resistance. The EDX spectra also revealed the effectiveness of APSA as a functional material in reducing the adhesion of scalants onto the membrane surface.

Lee et al. [66] further explored the potential of silk fibroin, a protein-based biopolymer, as an antiscalting coating material to improve the surface characteristics of the PA layer through the introduction of hydroxyl groups. Fig. 6(c) illustrates that the deposition of silk fibroin could efficiently suppress gypsum scaling on the membrane surface. As a comparison, the carboxyl group of pristine PA is likely to form strong complexes with  $\text{Ca}^{2+}$  of gypsum and induce scale formation. As a result, silk fibroin-modified membranes exhibited five times lower irreversible scaling resistance compared to the pristine membrane over the three cycles of the 20-h scaling test.

Park et al. [74] capitalized on the biocidal properties of triclosan by immobilizing it on the surface of TFC membranes. This modification aimed to enhance the membrane's resistance to biofouling caused by *Pseudomonas aeruginosa*. The addition of triclosan led to a reduction in the antibacterial activity of TFC membranes, as evidenced by the

decrease in biofilm growth from 11.91 to 7.53  $\mu\text{m}$ . This could be explained by the antibacterial action mechanism, where triclosan disrupted the bacterial wall and cytoplasmic membrane, retarding biofilm formation. Further investigation showed that the biofouling effect was more pronounced on the pristine TFC membrane during a crossflow filtration of *Pseudomonas aeruginosa* ( $10^2$  CFU/mL), in which its normalized flux dropped by 40 % in contrast to 27 % of triclosan-modified TFC membrane throughout the 26-h filtration.

#### 4.1.2. Inorganic materials

Recent advances in nanotechnology enable the integration of inorganic nanomaterials to alter the surface properties of TFC RO membranes. Among various nanomaterials, graphene oxide (GO) emerged as a popular choice of functional materials due to its superior hydrophilicity and extremely fast water channels. Cao et al. [75] grafted GO on the PA surface of commercial RO membranes to render the membrane surface with better functionality against gypsum scaling. Their research findings demonstrated that grafting GO onto the PA surface effectively inhibited the deposition of gypsum. This inhibition was attributed to the strong electrostatic repulsive forces between the negatively charged gypsum particles and the membrane with GO grafting. Notably, the zeta

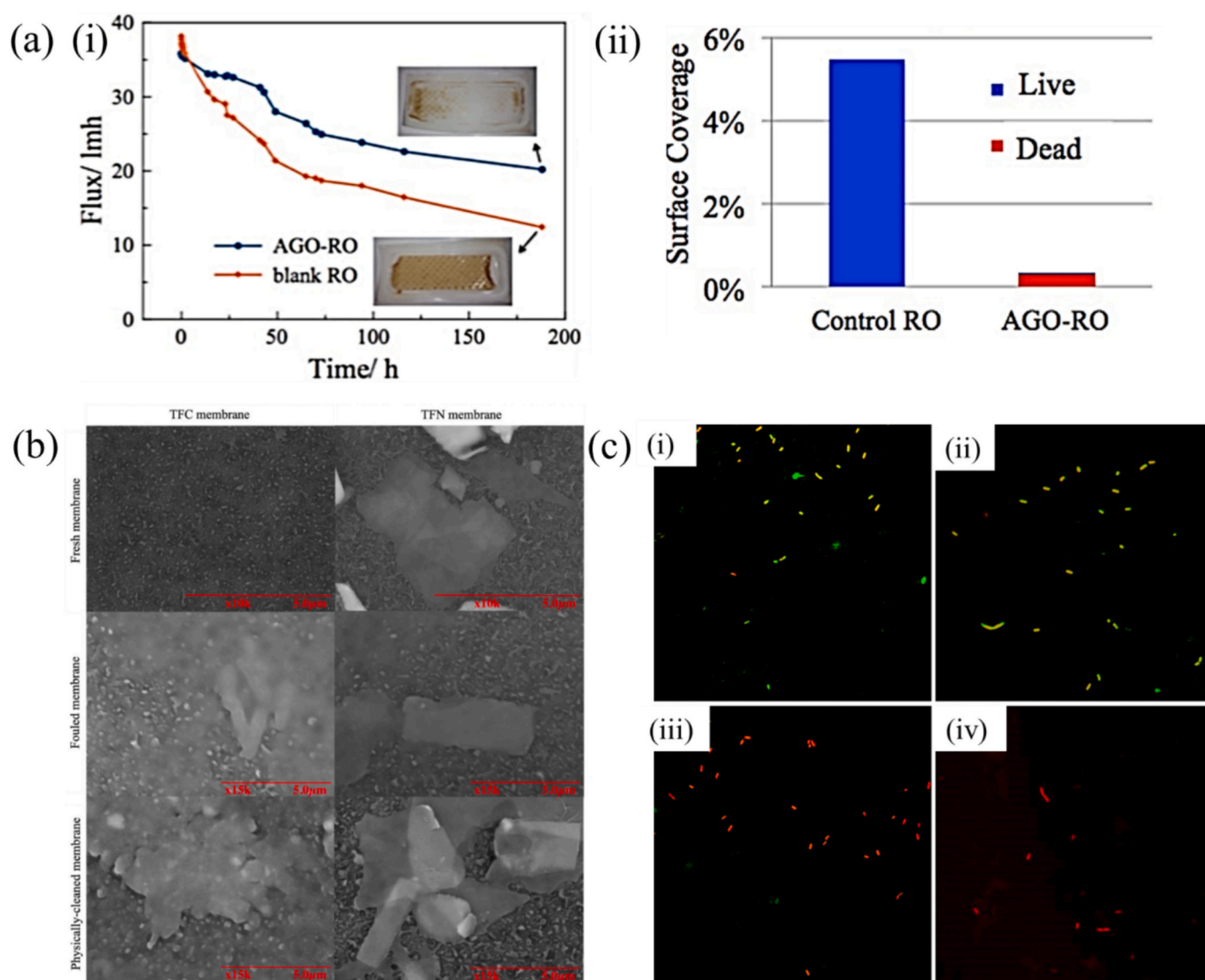


**Fig. 7.** (a) Performance of neat TFC and azide-functionalized GO: (i) flux decline during BSA fouling test and (ii) percentages of *E. coli* cells on the membrane surface [76], (b) SEM images of fresh, fouled and physically cleaned TFC and TNS-modified TFC membranes [77], and (c) CLSM images of *E. coli* (top) and *P. aeruginosa* (bottom) on the (i, ii) TFC and (iii, iv) Ag-modified TFC membranes (Note: live and dead cells are stained green and red, respectively) [78].

potential of the membrane at pH 5.8 was reported to decrease significantly from  $-20.8$  mV to  $-38.0$  mV upon grafting GO onto the PA layer. Consequently, the grafted membrane exhibited a lower degree of flux decline compared to the pristine membrane despite exhibiting similar initial fluxes during scaling experiments.

The incorporation of GO has also been verified to enhance the antibacterial properties of modified TFC membranes. Upon grafting of azide-functionalized GO onto the PA surface of the TFC membrane, Huang et al. [76] found that the GO-grafted TFC membrane could reduce *E. coli* biofouling up to 17 times after 24 h of contact. Only 0.32 % of the membrane surface was covered with *E. coli* (live and dead) as opposed to 5.46 % found on the control TFC membrane. In addition, the grafted TFC membrane was proven to display enhanced fouling resistance against BSA, recording approximately a 40 % flux decline compared to the 70 % recorded by the pristine membrane. Both membranes were tested with the same model solution for a duration of seven days (Fig. 7(a)). The improved surface smoothness of the grafted membranes was also observed to have a role in mitigating fouling. The lack of uneven surface characteristics such as valleys and ridges make it more challenging for protein particles to attach themselves to the membrane surfaces.

Employing the layer-by-layer (LbL) technique, Ahmad et al. [77] synthesized oppositely charged titania nanosheets (TNS) and assembled them atop a TFC RO membrane. At the optimum two bilayers of TNS coating, the resultant membranes showed excellent stability when subjected to a long-term antifouling study using a synthetic oily saline solution composed of 1000 ppm crude oil and 2000 ppm NaCl. The enhanced surface hydrophilicity of TNS-coated membranes coupled with its smoother surface led to a lower permeability decline (31.7 %) compared to the pristine TFC membrane (38.8 %). The improved surface features could reduce interaction between oil droplets and membrane surfaces. The extent of fouling was further evaluated in terms of irreversible fouling ( $R_{ir}$ ), where the presence of the TNS coating layer could lower the  $R_{ir}$  of the pristine membrane from 17.09 % to 6.12 %. Fig. 7(b) compares the SEM images between fresh, fouled, and water-cleaned TFC membranes. The foulants were visible in the neat TFC membranes even after physical cleaning, while the morphology of TNS-coated TFC membranes was restored upon cleaning with intact TNS coating.

The method of incorporating biocidal nanomaterials has been acknowledged as a promising approach for addressing biofouling. Silver (Ag) nanoparticles, with their wide-ranging biocidal properties and minimal cytotoxicity, have been extensively utilized to combat biofouling problems. Park et al. [78] employed an arc plasma deposition (APD) method to rapidly deposit Ag on the surface of commercial TFC RO membrane (SWC4+ from Nitto Denko). The strong antibacterial activity of the Ag-modified TFC membrane was confirmed by quantifying the number of colonies after contact for 2 h, in which the Ag-modified TFC membrane completely reduced the bacterial viability of *E. coli* and *P. aeruginosa* species, indicating its great ability to kill these microorganisms. Meanwhile, the pristine TFC membrane only demonstrated minor antibacterial properties with high bacterial viability of 95 % and 80 % for *E. coli* and *P. aeruginosa*, respectively. In addition to surface antibacterial action, the existence of Ag on the membrane could further inhibit bacterial intracellular metabolisms. As a result, all bacteria species on the Ag-modified TFC membrane were found to be dead, as evidenced by the red-stained cells in CLSM images in Fig. 7(c).

#### 4.1.3. Hybrid materials

Advancements in surface functionalization are paving the way for the exploration of new materials for modification. This includes the hybridization of organic and inorganic materials to fully unlock their potential in customizing the surface properties of TFC membranes. As mentioned in Section 4.1.2. Inorganic materials, the superiority of GO can be attributed to the presence of multiple oxygen-containing groups that allow for the attachment of more functional groups onto their surface without adversely affecting their structure. Taking advantage of

the hydrophilicity of GO and the adhesiveness of PVA, Ng et al. [79] established a hybrid coating layer composed of GO and PVA atop a PA layer of RO membrane and reported an improvement in the membrane fouling performance. The GO/PVA-coated TFC membrane could effectively recover 100 % of its initial permeability after being subjected to 5-h filtration using respective 1000 ppm BSA and 1000 ppm humic acid (HA) solution. The authors ascribed the enhanced antifouling characteristics to the expansion of the hydrophilic domain of the GO/PVA coating layer that promotes hydrogen bonding between water molecules and membrane surface, thus forming a hydrated layer that acts as a barrier that deterred direct adsorption of foulants on the membrane surface. Because of the strong interfacial interaction between GO and PVA, it was documented that the quantity of GO released from the membrane was exceedingly small and can be regarded as insignificant.

Aiming to reduce both biofouling and mineral scaling, Ansari et al. [80] synthesized an organic-inorganic (GO-PAA) grafting solution and used it to modify the surface of commercial RO membrane (ESPA2). The GO/PAA-modified TFC membrane experienced a slower flux decay rate ( $\sim 64$  %) compared to the neat ESPA2 membrane (78 %) during the gypsum scaling experiment conducted for 6 h. The heightened scaling resistance could be attributed to the increased surface hydrophilicity. According to the classic nucleation theory, a hydrophilic membrane lowers the liquid-substrate interfacial energy, which in turn increases the nucleation energy barrier, making gypsum nucleation on the membrane unfavorable. The authors further found out that the coverage of gypsum crystals on the neat membrane was greater and denser than the GO/PAA-modified membrane (see Fig. 8(a)). For the modified membrane, only certain parts of its surface were covered with biofilm. The improved surface hydrophilicity has also been shown to be beneficial in decreasing membrane biofouling susceptibility. This is because the hydrated layer acts as a barrier, preventing the attachment of bacteria to the membrane surface when a marine bacterial consortium is introduced into the feed solution. After washing the membranes at the end of the 48-h biofouling test, the higher normalized flux ratio of GO/PAA-modified membrane (0.90) indicated that the biofilm on the grafted membrane was easier to clean than the neat membrane (0.85).

Another study by Ahmad et al. [22] showed that the assembly of alternate layers of PEI and TNS via spray-assisted LbL can efficiently ameliorate membrane fouling resistance against organic foulants. During an extended filtration test using a 1500-ppm BSA solution for 8 h, the optimized PEI/TNS-assembled membrane exhibited a less significant decline in flux (20 %) when compared to the pristine TFC membrane (30 %). However, the authors observed more severe fouling when filtering 1500-ppm NaAlg solution, as loss of permeability reached 57 % and 27 % for the neat and PEI/TNS-assembled membranes, respectively. Due to the presence of multiple carboxylic acids, hydroxyl, and ether groups on NaAlg side chains, it possessed stronger interaction with the membrane surface through polar interaction. Nevertheless, the PEI/TNS-assembled membrane still exhibited superior fouling resistance as the loosely attached organic foulant can be easily cleaned from its surface and achieved 100 % flux recovery. Meanwhile, the TFC membrane exhibited FRR of 87 % and 70 % for BSA and NaAlg filtrations, respectively. As illustrated in Fig. 8(b), the authors explained that the greater antifouling performance can be conferred by two mechanisms, specifically fouling resistance and fouling release. The coating layer regulated foulants adhesion during filtration and facilitated its release from the membrane surface during cleaning.

A hybrid material consisting of organic-organic material has also shown promising results in mitigating surface fouling. In the study by Azmi et al. [81], an effort was made to graft the dipeptide consisting of the amino acid L-arginine, i.e., arginyl-arginine (Arg-Arg), onto the surface of TFC membrane. It was discovered that this approach effectively enhanced the membrane's antifouling properties, restoring up to 96.15 % of the initial flux after undergoing four cycles of filtration with a 2000 ppm BSA solution. Meanwhile, the TFC membrane was only able to recover 62.95 % of its permeability. The multiplication of functional

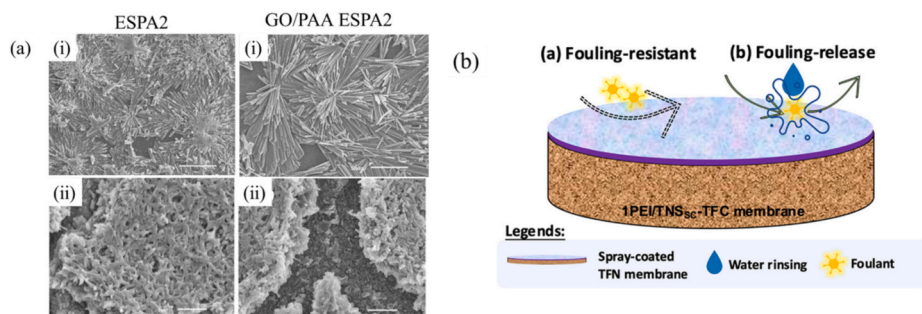


**Fig. 8.** (a) SEM images of (i, ii) gypsum scaled and (iii, iv) bio-fouled surfaces of ESPA2 and GO/PAA-modified ESPA2 membranes [80] and (b) Illustration of antifouling strategies by fouling resistance (preventing foulants from attracting to the membrane surface) and fouling release (weakening the interaction between foulant and membrane surface) [22,23].

groups of Arg amino acid to form Arg-Arg dipeptide through a facile grafting approach increased membrane surface smoothness and led to fewer adhesion sites for the attachment of hydrophobic BSA. On the other hand, Hu et al. [82] reported improved resistance against organic fouling and inorganic scaling when they grafted PEI and 2-bromoethanesulfonic acid (2-BES) on the TFC membrane. In a fouling performance test using CTAB as the model foulant, the TFC membrane grafted with PEI/BES demonstrated a lower flux decline of 42.3 %, as opposed to the pristine TFC membrane, which exhibited a higher flux decline of 50.7 %. The synergistic effects of the hybrid PEI/BES also demonstrated a significant impact on membrane anti-scaling performance, where the TFC membrane grafted with PEI/BES displayed a lower flux decline (32.3 %) compared to the neat membrane (48.3 %).

Wang et al. [84] utilized the emerging antimicrobial agent tobramycin (TOB) in conjunction with PAA to modify commercial RO membranes, to address and improve their biofouling issues. The establishment of negatively charged PAA and positively-charged TOB bilayer atop the RO membrane was found to be effective in achieving an almost complete bacteria mortality rate (99.6 %) against *B. subtilis* and *E. coli* owing to the cell lysis effect of TOB. As a comparison, the control membrane only showed a 10–15 % mortality rate. Moreover, the modified membrane also demonstrated a notable enhancement in anti-fouling performance during the filtration process with both BSA and NaAlg solutions.

The enhanced organic and biofouling attributes of TFC membranes modified by TOB prompted the authors to further enhance the feasibility of TOB as functional material by grafting it on TFC membrane together with 2,2,3,4,4,4-hexafluorobutyl methacrylate (HFBM) with the assistance of UV irradiation [86]. The realization of the triple antifouling strategy relies on three antifouling attributes fouling release, fouling resistance, and contact killing, brought by the synergistic effects of low-surface-energy HFBM brushes and hydrophilic TOB segments. After completing three cycles, each involving 4-h filtration of a 200 ppm BSA and 2000 ppm NaCl solution, the modified TFC membrane was able to recover up to 96.5 % of its initial flux, whereas the unmodified TFC membrane could only restore 48.1 % of its flux. The triple modification strategy was also found to endow the modified membrane with potent antimicrobial activity with a mortality higher than 99.8 % for both *E. coli* and *B. subtilis* species. The triple modification strategy was also discovered to impart the modified membrane with potent antimicrobial activity, resulting in a mortality rate exceeding 99.8 % for both *E. coli* and *B. subtilis* species. In contrast, the virgin TFC membrane exhibited an extremely low mortality rate (7.5 % for *E. coli* and 5.5 % for *B. subtilis*), which can be attributed to bacterial adhesion on its surface. Table S1 summarizes the performance of TFC RO membranes both before and after surface modification using various strategies, which include organic materials, inorganic materials, and hybrid materials. These modifications aim to enhance the membrane's resistance to fouling and scaling.

#### 4.2. Bulk modification of the PA layer of the RO membrane

Besides modifying the top surface of an existing PA layer, bulk PA modification is also employed to improve the fouling and scaling resistance of TFC RO membranes. In the following sections, we will examine the impact of three primary categories of materials used for bulk modification of the PA layer.

##### 4.2.1. Organic materials

Over recent years, biomaterials such as amino acids have been regarded as a new class of antifouling materials due to their superior hydrophilicity that can exhibit antiadhesion properties against foulants. Taking advantage of the hydrophilicity and the anionic features of L-lysine, Xu et al. [87] immobilized the amino acid into the PA layer via the MPD aqueous solution to develop a TFC membrane that demonstrated a stable performance during filtration of colloidal silica solution. As shown in Fig. 9(a), the TFC membrane with 0.3 wt% L-lysine exhibited a slower flux decline (21.9 %) compared to the neat TFC (27.3 %) and TFC membrane with 0.1 wt% L-lysine (24.2 %). Meanwhile, the recovered flux of the L-lysine-modified membrane after washing was slightly enhanced in comparison to the unmodified membrane, increasing from 81.5 % to ~85 %. This improvement can be attributed to the presence of carboxyl groups of L-lysine that effectively boost membrane colloidal fouling resistance by both hydrophilicity and electrostatic repulsion.

L-arginine is another biomolecule that consists of hydrophilic groups such as  $\alpha$ -carboxyl,  $\alpha$ -amino, and a complex guanidine that has distinct steric hindrance capable of reacting with acyl chloride groups. Therefore, its addition during the IP process could produce a highly hydrophilic selective layer, which in turn would minimize protein adhesion to the membrane surface during the filtration process. By adding 0.5 wt% L-arginine into MPD aqueous solution, Chen et al. [162] reported the water contact angle of the resultant membrane decreased from 76.9° to 51.3°, signifying enhanced affinity between membrane and water. This can be attributed to the abundance of carboxyl groups that form hydrogen bonds with water molecules. The increased surface hydrophilicity played a substantial role in recovering the initial flux and preventing significant flux decline during 10-h filtration using a feed solution composed of 1000 ppm BSA and 2000 ppm NaCl. Upon the L-arginine incorporation, the flux decline of the membrane decreased from 12.6 % to 8.1 %, while the FRR improved from 90.7 % to 96.2 %.

In 2023, Chen et al. [163] used L-arginine to co-polymerize with PDA nanoparticles and studied the dynamic alterations of its addition to the PA layer. They discovered that the inclusion of arginine and PDA introduced anionic carboxyl groups, which attracted the cationic MPD monomer, thereby expanding the reaction region at the aqueous-organic interface. Consequently, a significant amount of arginine-doped PDA was located on the front surface of the fabricated PA layer, as illustrated in Fig. 9(b). The resultant membrane was found to display a denser front surface and loose PA interior structure. This morphology is beneficial in

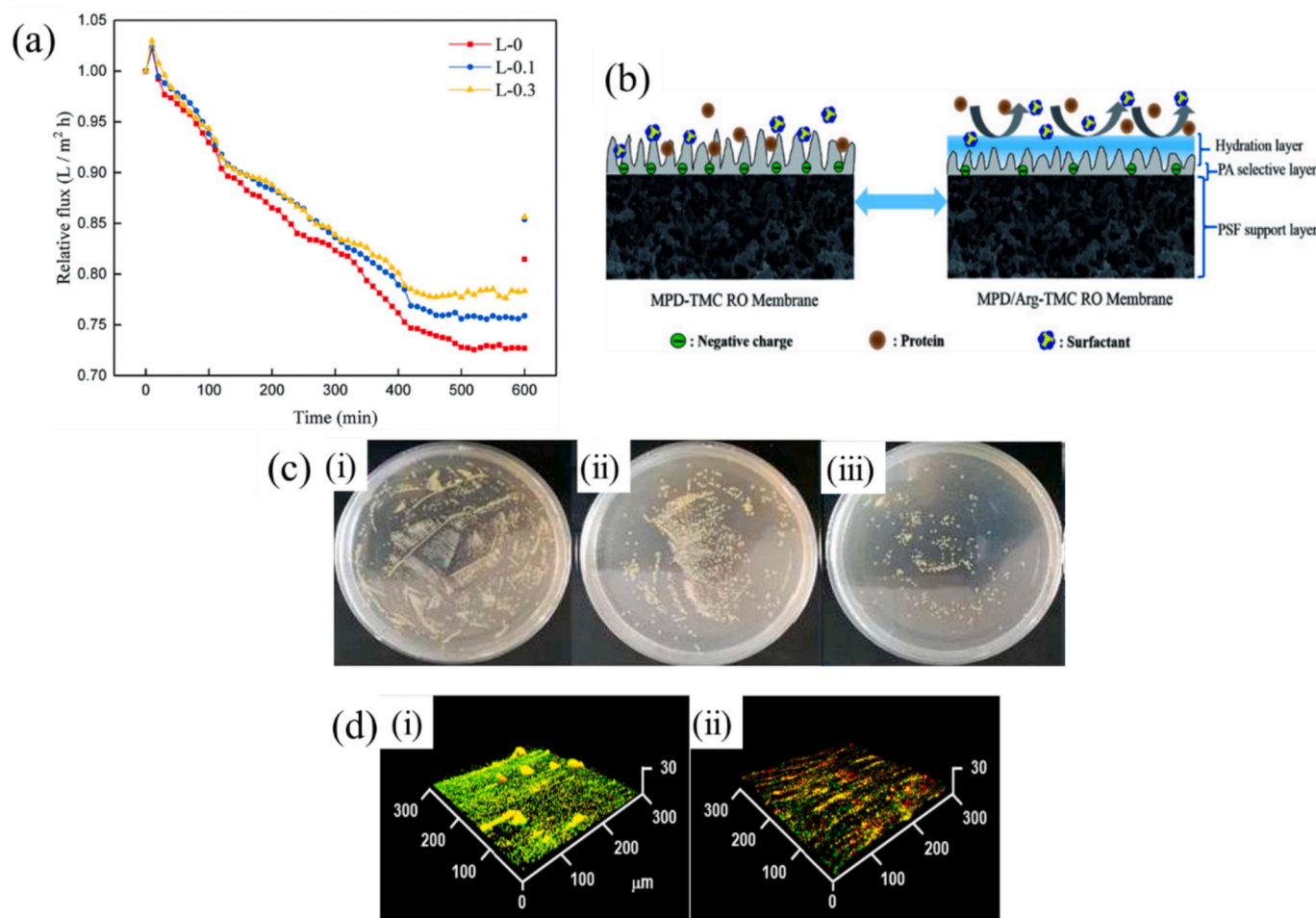


**Fig. 9.** (a) Time-dependent relative flux of neat TFC (L-0) and TFC incorporated with 0.1 wt% (L-0.1) and 0.3 wt% (L-0.3) of L-lysine during filtration of 500-ppm colloidal silica solution [87], (b) Illustration of the antifouling mechanism of L-arginine-functionalized TFC membrane [162], (c) *E. coli* colonies after being contacted with (i) blank, (ii) TFC, and (iii) PPy-functionalized TFC membrane [165], and (d) CLSM images of (i) TFC and (ii) peptoid-modified TFC membranes [166].

maintaining flux stability during long-term filtration of feed solution containing BSA (1000 ppm) and NaCl (2000 ppm). The TFC membrane with arginine-doped PDA experienced a flux decline of 7.2 % throughout the 20-h test compared to the control TFC membrane recorded 18.7 %. The enhanced surface hydrophilicity, attributed to the higher presence of carboxyl groups, also contributed to increasing the FRR from 87.2 % to 94.6 %.

Aside from protein, cellulose nanocrystals (CNC), which are synthesized by acid treatment of native cellulose, have also been used as a biodegradable modification material due to their low environmental impact. Its incorporation into the PA layer was first reported by Asempour et al. [164], to produce a TFC membrane capable of resisting organic fouling. Throughout the 20-h filtration using a feed composed of 300 ppm BSA and 3000 ppm NaCl, the water flux of the CNC-modified TFC membrane only dropped 15 % of its original flux, while the neat TFC membrane suffered from a 26 % flux increase. The authors attributed the reduced fouling propensity of the functionalized TFC membrane to increased surface hydrophilicity, resulting from the hydroxyl-rich CNC. This was evidenced by a decrease in the contact angle from 73.5° to 55.1°.

To elevate microbial resistance of the TFC membrane, Liao et al. [165] added biocidal polypyrrole (PPy) nanosphere into the organic phase solution during the IP reaction. Compared to many inorganic nanofillers, PPy is more cost-effective and biocompatible. Its organic nature promotes miscibility with polymer matrix. Most importantly, the positive surface charge of the PPy nanosphere could inhibit the growth of *E. coli* atop the TFC membrane. As shown in Fig. 9(c), the growth of

*E. coli* colonies on the 0.006 wt% PPy-modified TFC membrane was visibly reduced compared to the control TFC membrane. In terms of mortality rate, the PPy-functionalized TFC membrane recorded 89.14 % bacterial death which was significantly higher than the control TFC membrane of 66.91 %. This can be explained by the cationic property of PPy that disrupts the negatively charged cytoplasmic membrane of the adsorbed cell, causing leakage of internal nutrients and compositions, and resulting in imminent death.

Biomimetic peptides, which are composed of N-substituted glycines, can mimic the antimicrobial properties of natural peptides. In the work of Park et al. [166], the peptoid-functionalized TFC membrane was developed which exhibited lower flux decline and remarkably higher rinsing-induced FRR efficiency compared to the commercial SWC4+ membrane and the pristine TFC membrane synthesized. This highlighted its high propensity for biofouling during the filtration of feed-water containing *P. aeruginosa*. The cationic moiety and hydrophobic lipid chain of peptoids played a collective role in causing cell death. The biofouling resistance of the peptoid-functionalized TFC membrane was further confirmed through the CLSM analysis as shown in Fig. 9(d). The results revealed low biofilm formation with a large number of dead bacteria (stained red), as opposed to the extensive biofilm coverage on the neat TFC and SWC4+ membranes composed mainly of live cells (stained green).

By dispersing 2-methylimidazole (Hmim), an imidazole derivative, in the aqueous solution, Fei et al. [167] successfully improved the morphology of the resultant active layer by increasing the number of free-volume elements. The participation of Hmim in the IP process

causes a disturbance at the aqueous/organic interface, where it competes with MPD molecules to react with TMC and generate unstable molecular-scale N-acyl imidazole that is prone to hydrolysis. This leads to the formation of angstrom-scale free volumes as well as the generation of carboxyl groups that greatly enhance membrane hydrophilicity. When tested with 500 ppm BSA feed solution for 6 h, the Hmim-functionalized TFC membrane experienced only a 24.9 % flux decline compared to the 35.2 % exhibited by the neat TFC membrane. The modified TFC membrane also showed 14.9 % higher FRR than the control TFC membrane, recording 85.1 %.

#### 4.2.2. Inorganic materials

Recently, many studies have explored the potential of 2D nanomaterials as nanofillers in altering the bulk properties of the PA layer of TFC membranes. Typically, nanomaterials improve membrane properties through their superior hydrophilicity, high specific surface area, and nanochannels. Aside from the widely-used GO nanosheets, other emerging 2D nanomaterials that have gained immense tractions from membrane researchers are molybdenum disulfide ( $\text{MoS}_2$ ) and transition metal carbonitrides MXenes ( $\text{Ti}_3\text{C}_2\text{T}_x$ ) [168].

Li et al. [169] employed  $\text{MoS}_2$  nanosheets as an inorganic nanofiller

and studied their influence on the antifouling propensity of the resultant TFC membrane. During the first 3 h of the organic fouling test with a feed containing 100 ppm BSA and 2000 ppm NaCl, the TFC membrane lost 10 % of its initial water flux, whereas the  $\text{MoS}_2$ -modified membrane only lost 5 %. The well-distributed  $\text{MoS}_2$  nanosheets in the PA matrix as well as its electronegativity behavior effectively repulse BSA away from the membrane surface, thereby rendering the membrane with superior fouling resistance. As a result, the  $\text{MoS}_2$ -modified membrane demonstrated much more stable flux performance compared to the neat membrane during a fouling test lasting 14 h.

Wang et al. [170], on the other hand, synthesized  $\text{Ti}_3\text{C}_2\text{T}_x$  MXene of 3–4 layers with 3.5 nm in bulk thickness before incorporating it (0.015 wt%) into MPD aqueous solution for PA layer fabrication. The result showed that the developed membrane exhibited a smoother surface as the surface roughness of the control membrane was reduced greatly from 287.3 nm to 90.0 nm after the MXene incorporation. It is acknowledged that a smoother membrane surface could impose a better antifouling tendency [171]. Based on the SEM analysis, the amount of BSA attachment was lesser in the MXene-modified membrane compared to the unmodified membrane (Fig. 10a). Further investigation confirmed the role of MXene in minimizing the membrane flux

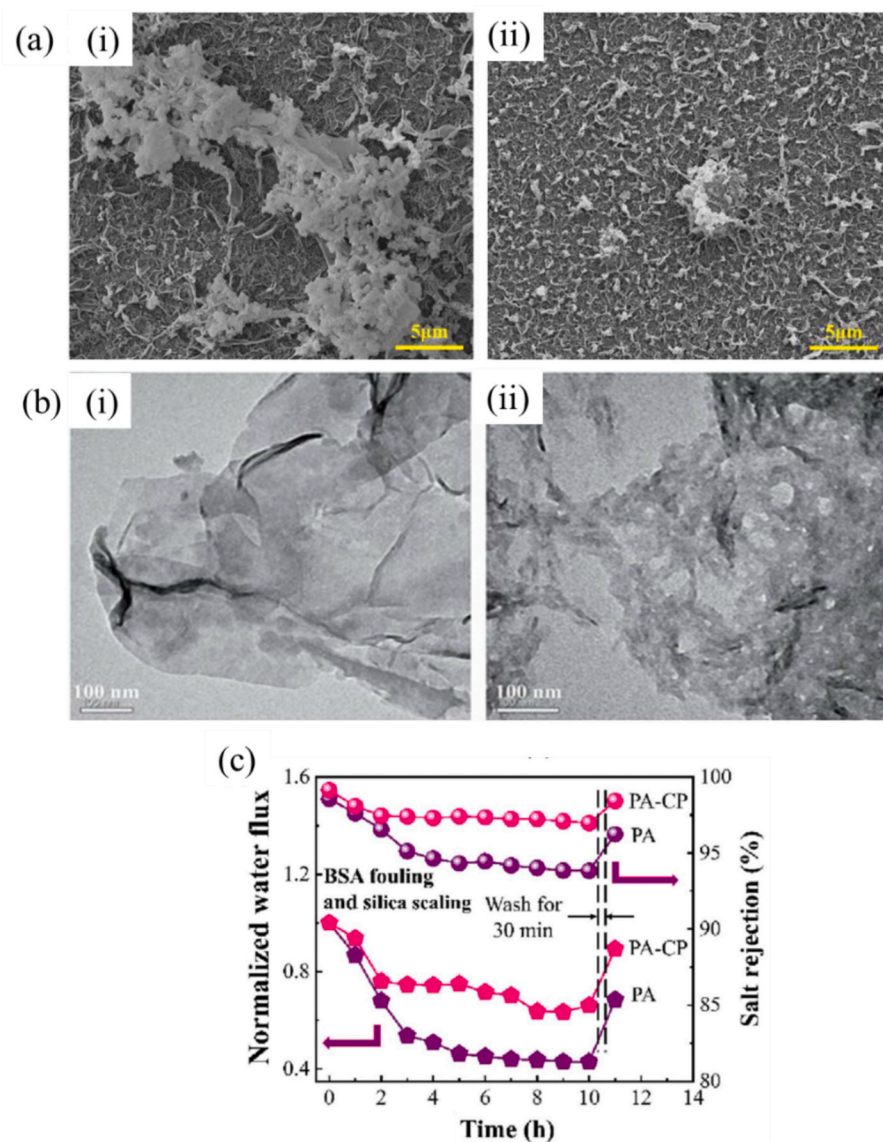


**Fig. 10.** (a) SEM images of (i) neat TFC membrane and (ii) MXene-modified TFC membrane after BSA fouling test [170], (b) TEM images of (i) gCN and (ii) aCN [160], and (c) Normalized water flux and salt rejection of TFC and g-C<sub>3</sub>N<sub>4</sub>/PPy-modified TFN membranes under combined BSA and silica fouling performance [174].

deterioration while maintaining an excellent salt rejection.

Another type of emerging 2D nanomaterial and an analog to graphene is boron nitride (BN). BN is well-known for its high resistance towards chemical oxidation which is an important characteristic of RO membrane. The addition of BN during the IP reaction can develop a thinner PA layer (>30 % reduction in thickness) owing to the slower migration of MPD from the aqueous to the organic phase region due to the uniform dispersion of BN in the aqueous solution [172]. Despite the rougher selective layer caused by the presence of BN nanosheets, which could trap foulants, the abundance of amine groups on the BN surface forms a water hydration layer that prevents foulant adhesion. Wang et al. [172] reported that in addition to a higher FRR, the BN-modified membranes also exhibited a 25 % higher water permeance compared to the pristine membrane, benefiting from its thinner PA active layer.

As a promising 2D graphene-like material, extensive studies are reporting the use of graphitic carbon nitride (g-C<sub>3</sub>N<sub>4</sub>) in membrane modification. g-C<sub>3</sub>N<sub>4</sub> possesses a defect-rich structure that shortens the solute transport path, permitting it to be more water permeable. However, g-C<sub>3</sub>N<sub>4</sub> has limited dispersibility in both aqueous and organic solutions, thus requiring functionalization before it is incorporated into the TFC membrane. Gao et al. [160] used sulfuric acid to oxidize g-C<sub>3</sub>N<sub>4</sub>, forming acidified g-C<sub>3</sub>N<sub>4</sub> (aCN) with artificial nanopores. The existence of nanopores was visualized in Fig. 10(b). When the aCN was incorporated into the PA active layer, it helped alleviate fouling resistance against BSA. Results indicated that the aCN-functionalized membrane showed better antifouling capacity ( $R_f$ : 34.7 % and FRR: 86.2 %) than the neat TFC membrane ( $R_f$ : 47.5 % and FRR: 71.3 %).

Aside from organic fouling, the potential of gCN nanosheets as functionalization material for TFC RO membrane has also been explored in an environment of combined organic and inorganic foulants. To further enhance the compatibility of g-C<sub>3</sub>N<sub>4</sub>, Ge et al. [174] grafted the

inorganic nanomaterial with PPy to create highly hydrophilic g-C<sub>3</sub>N<sub>4</sub>/PPy composites. At an optimal concentration of 0.005 wt%, the modified membrane displayed a 50 % reduction in PA thickness compared to the unmodified membrane due to a faster diffusion rate of MPD aqueous monomer into the organic phase in the presence of g-C<sub>3</sub>N<sub>4</sub>/PPy. The thinner active layer resulted in a fourfold increase in water permeability (from 1.06 to 4.00 L/m<sup>2</sup>·h·bar) while simultaneously improving NaCl rejection (from 98.6 % to 99.1 %). When the modified membrane was tested against a mixed feed solution containing BSA, Na<sub>2</sub>SiO<sub>3</sub>, CaCl<sub>2</sub>, and MgCl<sub>2</sub> for a duration of 10 h (see Fig. 10(c)), it only recorded a normalized flux decline rate of 0.34, significantly lower than the neat membrane that displayed 0.58. This is owed to the enhanced hydrophilicity brought by the presence of g-C<sub>3</sub>N<sub>4</sub>/PPy composites that heighten the energy barrier of the membrane surface for mineral scaling nucleation, thus reducing inorganic fouling adhesion onto the membrane.

#### 4.2.3. Hybrid materials

Although the potential of metal biocides such as Ag<sup>+</sup> and Zn<sup>2+</sup> in improving the antibacterial capacities of the TFC membranes has been explored [67,175], these metal ions often suffer from inevitable release that results in unstable performance [177]. To enhance long-term stability, the metal ions are often combined with other materials such as GO [178,179] and CNTs [10]. Li et al. [181] utilized Laponite (Lap), a synthetic silicate 2D nanoclay, as a metal ion carrier for Ag<sup>+</sup>, Cu<sup>2+</sup> and Zn<sup>2+</sup> via an ion exchange method. The newly developed Lap-mediated metal ion composites were then added into the aqueous solution at a concentration of 0.2 mg/mL to assess their effectiveness as bactericidal functionalization materials for the membranes. The antibacterial properties were investigated using *E. coli* and *S. aureus* as model bacterial strains after 2 h of exposure. As shown in Fig. 11(a), the neat TFC

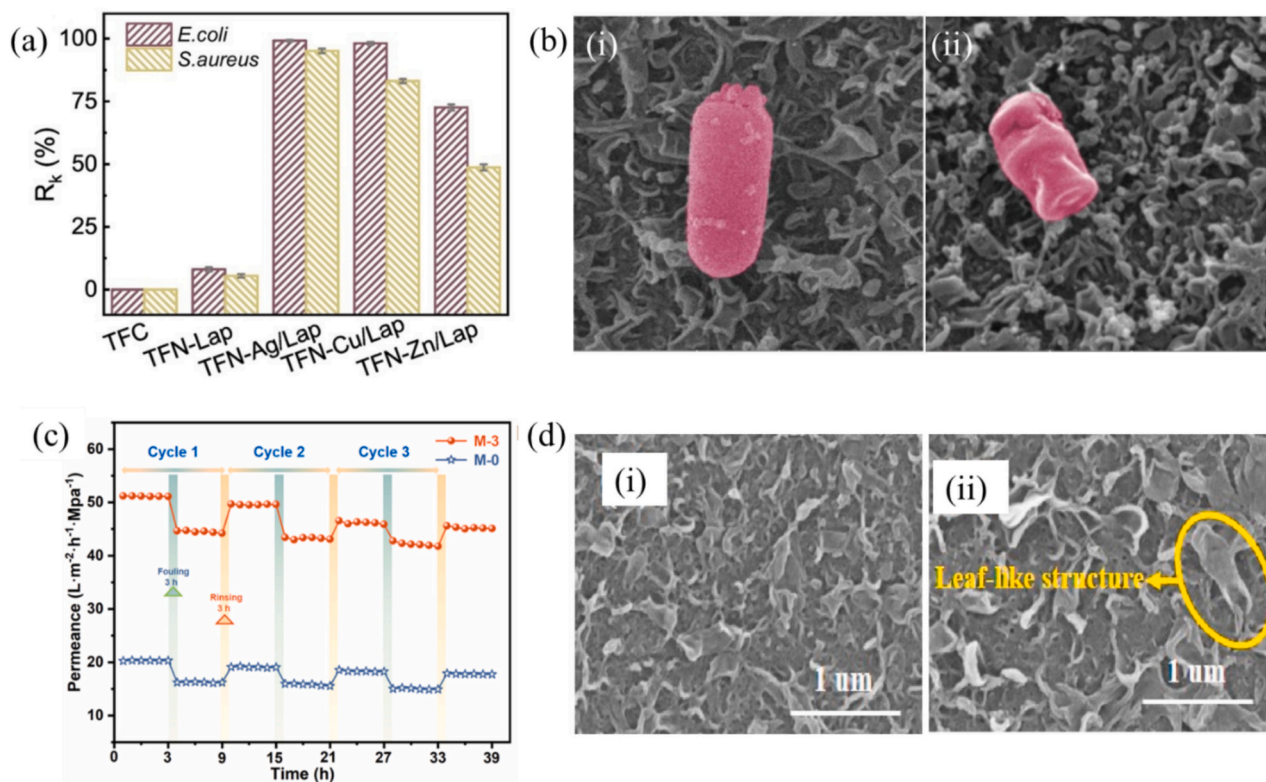


**Fig. 11.** Bactericidal rates of pristine TFC membrane and laponite-modified TFN membrane with varying types of metal ion carrier against *E. coli* and *S. aureus* [181], (b) SEM images of *E. coli* treated with (i) TFC membrane and (ii) TFN-Ag/Lap membrane [181], (c) water permeability of neat TFC membrane and MOF-modified TFN membrane during 3-cycle filtration of HA fouling test (Liu et al., 2022), and (d) Surface SEM images of (i) TFC and (ii) 0.005 wt% PANI/PPy-modified TFN membrane (Dong et al., 2022).

membrane showed a low bacteriostasis rate ( $R_k$ ) at 0 % for both bacteria, while the membrane with bare laponite demonstrated slightly higher  $R_k$  of 8.1 % and 5.5 % for *E. coli* and *S. aureus*, respectively. The authors attributed the improved properties to the enhanced membrane hydrophilicity due to Lap addition that weakens the adsorption of bacteria on the membrane surface.

Li et al. [181] also reported that the bacteria mortality rate improved exponentially after contact with the membrane containing various Lap-mediated metal ions, where the antibacterial activities increased in the order of TFN-Zn/Lap ( $R_k$ : 72.6 % and 48.7 %) < TFN-Cu/Lap ( $R_k$ : 98.1 % and 83.1 %) < TFN-Ag/Lap ( $R_k$ : 99.2 % and 95.1 %). This proved that the antibacterial properties of the functionalized membranes largely contributed to the interactions between the metal ions released from Lap composite and bacteria that increase oxidative stress in bacterial cells and damage both the cell membranes and proteins. The morphological changes of *E. coli* cells on the membranes were further examined by SEM, where a viable and intact *E. coli* cell was detected on the TFC membrane (Fig. 11(b)). In contrast, the *E. coli* adhered to the surface of the TFN-Ag/Lap membrane has a wrinkled structure, signifying cell damage or death.

Leveraging the biocidal properties of Ag, Wang et al. [44] decorated the surface of carboxyl-modified carbon nanospheres with Ag (CNs-COOH/Ag) before integrating them into the active layer of the TFC membrane. While the TFC membrane recorded no antibacterial activity (~0 %), the modified membrane with CNs-COOH/Ag exhibited an antibacterial efficiency of 93.5 %. The  $Ag^+$  ions released from CNs-COOH/Ag composite were credited with destroying bacterial metabolic activity due to their high affinity for thiol groups on the cell membrane. On the other hand, the carboxyl groups played a main role in simultaneously increasing surface hydrophilicity and reducing surface roughness, preventing the deposition of HA onto a membrane and enhancing its reusability. HA is a model foulant that represents a major component of natural organic matter in water sources. Evidently, after four cycles of HA filtration, the water permeance of the CNs-COOH/Ag-functionalized membrane decreased by only 16.8 %, while the bare TFC membrane recorded a flux decline of 23.8 %.

Metal-organic framework (MOF) is another nanomaterial that has garnered considerable attention in water and wastewater treatment. This is attributed to its crystalline and porous structure, consisting of metal ions interconnected by coordinating organic ligands. This arrangement enables excellent compatibility with polymeric membranes [183]. Liu et al. [184] introduced 0.015 wt% of nickel-based MOF to the MPD solution and found that its 2D hollow structure which is rich in hydrophilic groups provides more channels for water diffusion. This enhancement led to improved durability of the resultant membrane during three cycles of 500 ppm HA antifouling tests, lasting for 39 h as shown in Fig. 11(c). Conversely, Aljundi [185] also observed enhanced antifouling resistance by employing ZIF-8, which is a subclass of MOF, in the filtration of 100 ppm BSA, where the synthesized membrane experienced 13 % flux loss compared to the pristine TFC membrane that lost 53 % of its initial flux after 3.5 h.

In a separate study, Dong et al. [186] synthesized hollow mesoporous nanospheres using two different organic materials, i.e., polyaniline (PANI) and PPy before introducing them as nanofillers for membrane fabrication. Due to its hollow structures, mesoporous shell, and amino groups, the water pathway is shortened, thus promoting rapid transmission of water molecules. Furthermore, the presence of amino groups could bond with the PA layer and boost the inherent hydrophilicity of the modified membrane. The water contact angle of the membrane decreased significantly from 60° to 35°. The enhanced hydrophilicity also positively affected the organic fouling resistance of the membrane against HA with a lower flux decline rate recorded. Concerning morphology, the presence of 0.005 wt% PANI/PPy nanospheres led to the formation of a larger leaf-like structure in the modified membrane compared to the bare TFC membrane, as seen in Fig. 11(d). These surface characteristics aided in deterring HA from adhering to the

membrane surface, thus endowing the membrane with enhanced fouling resistance.

## 5. Theoretical models in membrane fouling

As fouling remains an inevitable issue for RO membranes, various models have been proposed for predicting and understanding the interactions in a fouling phenomenon in an effort to improve its operation performances. The modeling approaches for fouling can provide useful information for membrane operation and optimization depending on the nature of foulants and operational conditions. Some of the commonly used models for membrane organic and inorganic fouling include the blocking filtration model, resistance-in-series model, Derjaguin-Landau-Verwey-Overbeek (DLVO) theory, and Gibbs free energy models.

The classic blocking filtration model proposed by Hermans [88] and further developed by Hermia [89], interprets the physical mechanism of pore blockage, which consists of four distinctive mechanisms: complete blocking, intermediate blocking, standard blocking, and cake filtration. The complete pore blocking assumes that each solute particle blocks only one pore, preventing other particles from entering, while the intermediate pore blocking model considers the possibility of multiple particles blocking the same pore. On the other hand, standard blocking assumes that smaller particles can enter pores and reduce the pore volume as they accumulate. Cake or gel layer formation occurs when larger particles deposit on the membrane surface without blocking pores, either because the membrane has no pores or the pores are already blocked. The equations (Eqs. (1)–(4)) corresponding to each of these fouling mechanisms are listed as follows:

$$K_b \bullet V = J_{p0} \bullet (1 - e^{-K_b \bullet t}) \quad (1)$$

$$K_i \bullet V = \ln(1 + K_i \bullet J_{p0} \bullet t) \quad (2)$$

$$\frac{K_s \bullet t}{2} = \frac{t}{V} - \frac{1}{J_{p0}} \quad (3)$$

$$K_c \bullet V = \frac{2t}{V} - \frac{2}{J_{p0}} \quad (4)$$

where  $K_b$ ,  $K_i$ ,  $K_s$ , and  $K_c$  indicate complete blocking, intermediate blocking, standard blocking, and cake formation, respectively.  $J_{p0}$  refers to the initial permeate flux and  $K$  is a constant that represents the fouling rate.

Ochando-Pulido et al. [90] utilized the blocking filtration model to analyze the dynamic mechanisms during the final purification process of secondary-treated olive mill wastewater by using a commercial TFC RO membrane (BW30LE). They found that the formation of the cake layer was the dominant fouling mechanism during a steady-state operation, while its initial flux drop was due to concentration polarization. They also reported that the partial blocking model accurately described the incipient fouling formation on the membrane. This emphasized the importance of fouling models in understanding foulant behavior to maintain stable performance in large-scale filtration operations.

The Gibbs free energy thermodynamic model in the Derjaguin-Landau-Verwey-Overbeek (DLVO) theory has been widely used to calculate the energy of adhesion between foulant and membrane to predict whether a foulant will attach to the surface or be repelled, as shown Eq. (5), where it considers the Lifshitz-van der Waals forces and electrostatic forces. A negative  $\Delta G$  value indicates spontaneous adhesion or attraction as the attractive forces dominate, while a positive value implies the repulsion of foulant from the membrane surface [91]. An extended version of the theory, namely XDLVO, takes into account the influence of short-ranged acid-base forces that arise from polar interactions between surfaces, as expressed in Eq. (6). In cases of moderate to high ionic strengths, electrostatic forces are considered negligible in

relation to surface free energy [92], simplifying the equation as shown in Eq. (7).

$$\Delta G = \Delta G_{LW} + \Delta G_{EL} \quad (5)$$

$$\Delta G = \Delta G_{LW} + \Delta G_{EL} + \Delta G_{AB} \quad (6)$$

$$\Delta G = \Delta G_{LW} + \Delta G_{AB} \quad (7)$$

where  $\Delta G$  is the total interfacial free energy between the membrane and the foulant species and  $\Delta G_{LW}$ ,  $\Delta G_{EL}$ , and  $\Delta G_{AB}$  represent the Lifshitz–van der Waals, electrostatic, and acid-base forces, respectively.

In Nguyen et al.'s [93] work, the researchers employed the XDLVO theory to determine the energetic interaction between foulant (NaAlg) and TFC membrane with and without PVA and zeolite coating. They obtained  $-14.7 \text{ mJ/m}^2$  for the uncoated TFC membrane and  $5.0 \text{ mJ/m}^2$  for the coated membrane. The results indicated that the modified membrane displayed lower fouling propensity compared to the pristine membrane. This was demonstrated by the improvement in flux decline after 28 h of filtering 100 ppm NaAlg. The PVA/zeolite-coated TFC membrane showed a lower flux decline rate (43 %) compared to the pristine TFC membrane (59 %).

Aside from that, an extended Young's equation has also been extensively adopted to determine surface tension parameters of membranes and foulants, in which it expresses the relationship between the contact angle of liquid on a solid surface and the surface tension parameters of both solid and liquid [92,94]. The surface energy of membranes is discerned by measuring the contact angles of at least two probe liquids with known liquid surface tension values ( $\gamma_1^{LW}$ ,  $\gamma_1^-$ ,  $\gamma_1^+$ ) and calculated using Eq. (8) [95]. The total surface energy of the membrane and between two phases (i.e., membrane-water, membrane-foulant, foulant-water) is then determined using Eqs. (9) and (10), respectively.

$$(1 + \cos \theta)\gamma_L = 2 \left( \sqrt{\gamma_m^{LW}\gamma_l^{LW}} + \sqrt{\gamma_m^+\gamma_l^-} + \sqrt{\gamma_m^-\gamma_l^+} \right) \quad (8)$$

$$\gamma_m = \gamma_m^{LW} + 2\sqrt{\gamma_m^+\gamma_l^-} \quad (9)$$

$$\gamma_{12} = \left( \sqrt{\gamma_1^{LW}} - \sqrt{\gamma_2^{LW}} \right)^2 + 2(\sqrt{\gamma_1^+} - \sqrt{\gamma_2^+})(\sqrt{\gamma_l^-} - \sqrt{\gamma_2^-}) \quad (10)$$

where  $\theta$  is the contact angle,  $\gamma_L$  is the total liquid surface tension,  $\gamma_{12}$  is the total surface tension between phase 1 and phase 2,  $\gamma^{LW}$ ,  $\gamma^+$ , and  $\gamma^-$  are the Lifshitz–van der Waals, electron acceptor, and electron donor components, respectively. The subscript  $m$  and  $l$  indicate membrane surface and liquid, respectively while 1 and 2 indicate the phases.

Jaramillo et al. [96] calculated the surface energy of a commercial BW30 membrane, both with and without a poly(sulfobetaine methacrylate) (PSBMA) zwitterionic brush coating, to assess its behavior during 48-h filtration of a 5000 ppm gypsum solution. The authors found that the zwitterion-coated BW30 membrane had a higher surface energy ( $70.1 \text{ mJ/m}^2$ ) compared to the control BW30 membrane ( $56.5 \text{ mJ/m}^2$ ), suggesting an improved capacity for water molecules to bind with each other—an important property for preventing scalant attachment. They also calculated the interfacial energy between membrane and gypsum ( $\gamma_{m-g}$ ), where the coated membrane achieved  $2.0 \text{ mJ/m}^2$ , an increase from  $-1.6 \text{ mJ/m}^2$  recorded by the control membrane. The positive interfacial energy indicated a lower tendency of gypsum crystal adsorption on the surface of the zwitterion-coated membrane. The results were consistent with the trend observed in gypsum scaling RO experiments, where the permeability of the zwitterion-coated membrane decreased by only 23.7 % from its initial flux after 48-h operation, compared to a 49.5 % flux decline for the control membrane.

Another thermodynamic model developed based on minimizing the Gibbs free energy called the nucleation model has contributed to determining the thermodynamic barrier of the crystal nucleation process. Essentially, there are two different nucleation pathways: homoge-

enous (bulk crystallization) and heterogenous (surface crystallization) [97]. Membrane surfaces generally stimulate heterogenous nucleation as they need lower free energy to overcome the nucleation barrier for crystallization growth. The critical free energy of heterogenous nucleation can be calculated using Eq. (11).

$$\Delta G_{cri} = f(\theta)\Delta G_{cri}^{hom} \quad (11)$$

where  $\Delta G_{cri}$  represents the critical free energy of heterogenous nucleation,  $f(\theta)$  is the correction factor or wetting function ( $f(\theta) = \frac{(2-\cos\theta)(1-\cos\theta)^2}{4}$ ), and acts as a function of the contact angle ( $\theta$ ) between the membrane and crystal nucleus.  $\theta$  is calculated using Young's equation that involves the interfacial free energy of the foulant, water, and membrane surface [98] as described by Eq. (12):

$$\cos\theta = \frac{\gamma_{m-l} - \gamma_{m-f}}{\gamma_{f-l}} \quad (12)$$

where  $\gamma_{m-l}$ ,  $\gamma_{m-f}$ , and  $\gamma_{f-l}$  denote the interfacial free energies associated with membrane-water, membrane-foulant, and foulant-water boundaries at thermodynamic equilibrium, respectively.

Meanwhile, the critical free energy homogenous nucleation can be calculated using Eq. (13):

$$\Delta G_{cri}^{hom} = \frac{16}{3}\pi \frac{\gamma_{f-l}^3 V^2}{[K_B T \ln(SI)]^2} \quad (13)$$

where  $V$ ,  $K_B$ ,  $T$ , and  $SI$  represent the molecular volume of foulant, Boltzmann constant, absolute temperature, and saturation index of foulant, respectively.

Khoo et al. [26] applied an acrylic acid coating layer over the titania nanotubes (TNT)-embedded PA layer of a TFC membrane to enhance surface hydrophilicity before conducting a 12-h silica scaling test. They used the wetting function,  $f(\theta)$ , to study the energy barrier of the fabricated membranes towards heterogenous silica nucleation and found that the modified TFC demonstrated larger  $f(\theta)$  value (0.92) than that of the neat TFC membrane (0.06). This suggested that silica nucleation is less likely to occur on membranes with enhanced hydrophilicity. The coated membrane also recorded higher surface energy ( $138.2 \text{ mJ/m}^2$ ) than the control membrane ( $97.7 \text{ mJ/m}^2$ ), confirming the potential of a higher energy barrier to reduce scale nucleation. Consequently, the coated membrane was able to recover 88.1 % of its initial flux after water rinsing, whereas the neat membrane achieved a flux recovery rate of 72 %.

## 6. Comparison of surface modification techniques and materials of TFC RO membranes

As discussed in Section 4, surface modification of TFC RO membranes has proven effective in enhancing fouling and scaling resistance. However, some modifications may compromise performance, potentially affecting permeability or rejection efficiency. In this section, we compare the filtration performance of selected TFC RO membranes before and after modification, as shown in Table S1 and Table S2. As seen, over half of the studies reported an improvement in membrane water permeability without compromising solute rejection. This is especially prominent in the TFC RO membranes modified by hybrid materials, where the synergistic approach of combining the functionalities of two materials significantly improves membrane surface properties. For instance, Dong et al. [99] applied a TA-Fe-PEI coating layer on the surface of a commercial TFC RO membrane (RE4021) and the resultant membrane outperformed the control membrane by showing an increase in permeability (from 2.95 to  $3.41 \text{ L/m}^2\cdot\text{h}\cdot\text{bar}$ ) and NaCl rejection (from 98.95 % to 99.18 %).

In addition to enhancing permeability or solute rejection, modifying the PA selective layer through coating, grafting, or LbL assembly has

been widely used to increase membrane resistance to fouling and scaling by improving surface hydrophilicity and charge properties. Among these strategies, surface coating is the most preferred method as it can effectively deposit a coating layer while maintaining the structural and chemical properties of the PA layer without any alteration. For instance, Jung et al. [101] coated the surface of the TFC membrane with silk sericin, rendering the top surface of the membrane with various hydrophilic amino acids and forming a thick hydration layer that could efficiently reduce gypsum scaling by increasing gypsum nucleation barrier. However, optimizing the coating layer is crucial, as several studies have reported reduced water permeability due to the presence of an additional layer, particularly when it is thick and dense, which increases water resistance [65,66]. Another concern is the weak interaction between the coating layer and the existing PA that might jeopardize its structural integrity during the long-term filtration process or aggressive membrane cleaning process [102].

Surface grafting is a technique that allows precise control in covalently bonding functional groups to the selective layer. Compared to surface coating, surface grafting is considered more chemically stable due to the strength of the covalent attachment [103]. Li et al. [104] grafted 3-sulfopropyl potassium methacrylate (SPM) onto the surface of a commercial TFC RO membrane (RO5). The grafted SPM was reported to increase membrane surface electronegativity, thus inhibiting the attachment of the combined NaAlg and silicate foulants by generating strong electrostatic repulsion. As a result, the SMP-grafted RO5 membrane retained 92 % of its initial flux after 150-min filtration. In contrast, the control membrane attained only 85 % of its flux. However, surface grafting often involves labor-intensive and time-consuming procedures that require the use of hazardous chemicals. To initiate a radical reaction to graft SPM, they utilized potassium persulfate ( $K_2S_2O_8$ ) and sodium metabisulfite ( $Na_2S_2O_5$ ) as redox initiators. Although both initiators are widely used to generate oxygen-centered radicals that facilitate monomer grafting, they pose a risk of causing severe irritation to the eyes, skin, and respiratory system and are classified under Category 1 according to the Globally Harmonized System (GHS). In addition, grafting processes such as plasma-induced technique are difficult to scale up and reproduce, as they require sophisticated equipment, thus unfeasibly increasing production costs [105].

Another preferred method of tailoring the existing PA surfaces of TFC RO membranes is the LbL method, which has brought substantial improvements as it enables fine-tuning of membrane performance by depositing multilayered polyelectrolyte complexes on the membrane surface. As most polyelectrolytes are water-soluble polymers, their deposition can endow the membrane surface with enhanced hydrophilicity that is beneficial in fouling and scaling resistance [106]. After assembling six bilayers of GO/TiO<sub>2</sub> on top of the TFC RO membrane via the LbL method, Shao et al. [107] reported improved antifouling properties of the modified RO membrane, attributed to enhanced surface hydrophilicity. It must be noted that the presence of GO/TiO<sub>2</sub> bilayers also acted as a sacrificial layer, protecting the underlying PA layer, when it was exposed to chlorine radicals. Nonetheless, the modification of TFC RO using the LbL method is often time-consuming as it involves multi-step coating procedures, especially when many layers are required. For example, the time taken to produce a six-bilayered GO/TiO<sub>2</sub> on the TFC RO membrane was 12 h, as the deposition of GO and TiO<sub>2</sub> required 1 h each. Another concern with bilayers is their stability, as the structure relies on the sequential deposition of oppositely charged polyelectrolytes, which can degrade, especially during long-term filtration of feed solutions with high salinity and ionic strength [108].

On the other hand, the bulk modification of the PA layer is an eye-catching procedure in engineering membrane surfaces to promote its resistance towards foulants and scalants. This is primarily due to its simple in-situ modification procedure, in which the modification materials can be directly introduced into the monomer solutions during the IP reaction. The presence of modification materials at the polymerization reaction zone could promote crosslinking between active monomers

by controlling their diffusion behavior. Vatanpour et al. [42] reported that incorporating 0.02 wt% titanium dioxide/carbon dots (TiO<sub>2</sub>/CDs) nanocomposite into the MPD aqueous solution inhibited the diffusion rate of MPD into the organic phase, resulting in a PA layer with reduced roughness and contact angle. This improvement contributed to maintaining a stable flux during the 12-h filtration process, showing a flux decline of 10 % compared to the 40 % decline observed with the unmodified membrane. However, the method of embedding modification materials into the PA layer still suffers from a persisting issue, which is the risk of poor dispersibility of materials in either aqueous or organic solutions, which could lead to the formation of surface defects in the PA film and adversely affect permeate quality [109]. As such, researchers often functionalize the materials before incorporating them into the PA layer to enhance their stability in the monomer solutions. However, this additional step may incur extra costs.

Over the last decade, a plethora of materials have been widely explored to modify the surface of TFC RO membranes to improve their intrinsic characteristics such as hydrophilicity, roughness, and surface charge, thereby increasing their resistance to fouling and scaling. Nonetheless, it is crucial to select materials carefully to engineer a modification layer with the desired properties. To date, endowing membrane surfaces with hydrophilic materials has been the most applied strategy in constructing TFC RO membranes with better resistance towards foulants/scalants.

Organic materials, characterized by their complex molecular structures and carbon-based backbones, offer a versatile platform for increasing surface hydrophilicity. For example, hydrophilic polymers such as PVA and PEG have been extensively utilized in TFC RO modification due to their water-soluble, neutrally charged, and hydroxyl-rich functional groups that are able to hinder the adsorption of hydrophobic foulants onto membrane surface [110]. In addition to the abundance of hydroxyl and amine groups, PDA, which is a bio-inspired polymer, has also been widely used primarily in the post-modification of TFC RO membranes. This is primarily attributed to its strong covalent and non-covalent interactions with membrane surfaces [72]. In addition to polymers, biomolecules such as proteins and carbohydrates provide unique functionalities for membrane modification, particularly in inhibiting microbial attachment and promoting bacterial cell death, thereby minimizing the biofouling phenomenon [85,86]. However, these organic materials tend to have limited thermal and chemical stability, and thus require proper handling. For instance, in the Lee et al. [111] study, the proteoliposomes must be stored at  $-80^{\circ}C$  before being encapsulated into the PA layer, and the resultant TFC membranes should be kept in deionized water at  $4^{\circ}C$  to prevent structural degradation.

In contrast, inorganic materials such as metal oxides (e.g., TiO<sub>2</sub> and ZnO) and carbon-based materials (e.g., GO and CNT) not only offer superior thermal and chemical stability compared to organic materials but also exhibit unique functionalities, such as photocatalytic effects. For example, the photocatalytic activity of TiO<sub>2</sub> can help in mitigating organic fouling and biofouling issues [112], while the inherent biocidal properties of Ag particles can significantly inhibit bacterial attachment to the membrane surface [113]. The wide utilization of two-dimensional GO in TFC RO modification can be attributed to its ultrathin structure and tunable nanochannels that are functionalized with multiple oxygen-rich groups that can greatly improve membrane hydrophilicity, thus assist in alleviating fouling/scaling [114]. Meanwhile, zeolites such as NaA and NaX provide a high surface area and tunable pore sizes and shapes, allowing for preferential flow paths for water permeation. This helps minimize concentration polarization near the membrane surface, which is a significant contributor to fouling and scaling. Another significant advantage of using inorganic materials compared to organic materials is that they are more cost-effective and easily obtained or produced. However, the primary challenge in modifying TFC RO membranes with inorganic materials is their high surface area and charge density, which can lead to agglomeration [115]. This compromises access to their active sites and may deteriorate the membrane's

integrity.

With the possibility of combining the synergistic strengths of organic and inorganic materials, hybrid materials have created a new paradigm in modifying TFC RO membranes that results in better surface properties. Compared to the incorporation of purely organic or inorganic materials, integrating hybrid materials offers improved tunability, as combining different materials allows for precise control over membrane properties. For instance, Hu et al. [82] grafted the organic-organic PEI/BES hybrids onto the TFC membrane surface to combine the fouling-resistant property of PEI and the repulsion ability of sulfonic acid of BES against silicic acid. The grafting was found to greatly improve membrane hydrophilicity from 60° to 27.2°, which led to slower flux decay during the filtration of both CTAB and gypsum. Despite their significant potential, hybrid materials also have drawbacks, primarily related to production costs. The complexity of synthesizing and manufacturing hybrid materials can result in higher production expenses, limiting their large-scale application and accessibility. Additionally, hybrid materials typically require more modification components than single organic or inorganic materials, which can make them less economically viable.

## 7. Conclusion

This review has been conducted to examine the advancements in RO membrane technology over the past decade, particularly concerning the persistent challenge of membrane fouling. Bibliometric analysis has illustrated a steady increase in research output, with significant contributions highlighted from nations such as China, the USA, South Korea, Australia, and Saudi Arabia. It is evident that the interactions between foulants and membranes are pivotal to the fouling process, with various membrane characteristics, including hydrophilicity, surface roughness, and functional groups, being influential, along with operational hydrodynamic conditions. A diverse range of materials, both organic and inorganic, has been investigated for their potential to enhance anti-fouling properties and improve overall membrane performance. Notably, materials such as graphene oxide, carbon nanotubes, and titanium dioxide have been shown to effectively reduce fouling and enhance membrane functionality. These developments are deemed crucial for advancing the efficiency of desalination technologies, particularly in light of the growing global concern regarding water scarcity.

Several theoretical models have also been discussed to further understand the behavior and interactions that occur during the fouling and scaling filtration process. The surface free energy theoretical model is one of the most important tools to determine the tendency of membranes prone to fouling and scaling. Meanwhile, the classic nucleation theory, particularly heterogenous nucleation, is another model theory that is useful in mitigating scaling by predicting the scaling tendencies and allowing for the development of strategies to prevent and minimize scaling on membrane surfaces.

The modification of TFC RO membranes, either through deposition on the existing PA layer or embedment within the PA layer during the interfacial polymerization process, has demonstrated significant potential in enhancing membrane performance, particularly in reducing fouling and scaling. While it is challenging to determine which modification strategy is the most effective for increasing membrane resistance to foulants, both approaches offer significant advantages in the context of large-scale industrial TFC membrane production. Modifying the top PA layer can be easily integrated into existing manufacturing lines, and the bulk modification of the PA layer involves a relatively straightforward procedure.

This review also compares the incorporation of organic, inorganic, and hybrid materials in modifying TFC RO membranes. Advances in material science have facilitated the development of functionalized RO membranes that can more effectively resist the accumulation of foulants, enhance water permeability, and prolong membrane longevity.

Compared to the incorporation of purely organic or inorganic materials, hybrid materials have been identified as more effective in enhancing membrane performance, thanks to the combination of functionalities from two or more different materials. Therefore, research on the development of TFC RO membranes modified with hybrid materials should be prioritized. Additionally, since most of the studies reported in the literature are primarily confined to lab-scale filtration tests, future research is recommended to conduct long-term filtration tests using real-life foulants encountered in practical applications.

## Declaration of competing interest

The authors declare that they have no known competing financial interests or personal relationships that could have appeared to influence the work reported in this paper.

## Acknowledgments

Open Access funding provided by the Qatar National Library.

## Appendix A. Supplementary data

Supplementary data to this article can be found online at <https://doi.org/10.1016/j.desal.2024.118508>.

## Data availability

No data was used for the research described in the article.

## References

- [1] Y. Wada, M. Flörke, N. Hanasaki, S. Eisner, G. Fischer, S. Tramberend, D. Wiberg, Modeling global water use for the 21st century: the water futures and solutions (WfAS) initiative and its approaches, *Geosci. Model Dev.* 9 (1) (2016) 175–222.
- [2] N.T. Thu, S. Patra, A. Pranudta, T.T. Nguyen, M.M. El-Moselhy, S. Padungthorn, Desalination of brackish groundwater using self-regeneration hybrid ion exchange and reverse osmosis system (HSIX-RO), *Desalination* 550 (2023) 116378.
- [3] M.Y. Ashfaq, M.A. Al-Ghouti, H. Qiblawey, N. Zouari, D.F. Rodrigues, Y. Hu, Use of DPSIR framework to analyze water resources in Qatar and overview of reverse osmosis as an environment friendly technology, *Environ. Prog. Sustain. Energy* 38 (4) (2019) 13081.
- [4] P.M. Biesheuvel, L. Zhang, P. Gasquet, B. Blankert, M. Elimelech, W.G.J. Van Der Meer, Ion selectivity in brackish water desalination by reverse osmosis: theory, measurements, and implications, *Environ. Sci. Technol. Lett.* 7 (1) (2019) 42–47.
- [5] C. Skuse, A. Gallego-Schmid, A. Azapagic, P. Gorgojo, Can emerging membrane-based desalination technologies replace reverse osmosis? *Desalination* 500 (2021) 114844 <https://doi.org/10.1016/j.desal.2020.114844>.
- [6] B. Mayor, Growth patterns in mature desalination technologies and analogies with the energy field, *Desalination* 457 (2019) 75–84.
- [7] L.A. Shouman, R.M. Afify, D.A. Fadel, M.H. Esawy, Fouling effect on reverse osmosis (RO) membranes performance in desalination plant, *Desalination and Water Treatment* 319 (2024) 100502, <https://doi.org/10.1016/j.dwt.2024.100502>.
- [8] Y. Chen, Y. Cohen, Calcium sulfate and calcium carbonate scaling of thin-film composite polyamide reverse osmosis membranes with surface-tethered polyacrylic acid chains, *Membranes* 12 (12) (2022).
- [9] T. Tong, A.F. Wallace, S. Zhao, Z. Wang, Mineral scaling in membrane desalination: mechanisms, mitigation strategies, and feasibility of scaling-resistant membranes, *J. Membr. Sci.* 579 (2019) 52–69.
- [10] S. Zhao, Z. Liao, A. Fane, J. Li, C. Tang, C. Zheng, J. Lin, L. Kong, Engineering antifouling reverse osmosis membranes: a review, *Desalination* 499 (2021) 114857.
- [11] M. Tawalbeh, et al., Engineering antifouling reverse osmosis membranes: a review, *Desalination* 591 (2023) 115274.
- [12] Q. Zhu, et al., Advances in antifouling techniques for reverse osmosis and forward osmosis applications, *Desalination* 530 (2022) 115689.
- [13] B.P. Ladewig, et al., Surface-modified membranes for biofouling mitigation in desalination: a review, *J. Membr. Sci.* 665 (2022) 120887.
- [14] R. Ullah, I. Asghar, M.G. Griffiths, An integrated methodology for bibliometric analysis: a case study of internet of things in healthcare applications, *Sensors* 23 (67) (2023), <https://doi.org/10.3390/s23010067>.
- [15] M. Kalantari, S.S. Moghaddam, F. Vafaei, Global research trends in petrochemical wastewater treatment from 2000 to 2021, *Environ. Sci. Pollut. Res.* 30 (4) (2023) 9369–9388.
- [16] L.D. Tijj, Y.C. Woo, J.-S. Choi, S. Lee, S.-H. Kim, H.K. Shon, Fouling and its control in membrane distillation—a review, *J. Membr. Sci.* 475 (2015) 215–244.

- [19] M. Filella, Colloidal properties of submicron particles in natural waters, in: IUPAC Series on Analytical and Physical Chemistry of Environmental Systems 10, 2007, p. 17.
- [20] M. Ponomarev, E. Krasnyuk, D. Butylskii, V. Nikonenko, Y. Wang, C. Jiang, T. Xu, N. Pismenskaya, Sessile drop method: critical analysis and optimization for measuring the contact angle of an ion-exchange membrane surface, *Membranes* 12 (8) (2022) 765.
- [21] C. Yang, M. Long, C. Ding, R. Zhang, S. Zhang, J. Yuan, K. Zhi, Z. Yin, Y. Zheng, Y. Liu, H. Wu, Z. Jiang, Antifouling graphene oxide membranes for oil-water separation via hydrophobic chain engineering, *Nat. Commun.* 13 (1) (2022).
- [22] N.A. Ahmad, P.S. Goh, K.C. Wong, S.C. Mamah, A.F. Ismail, A.K. Zulhairun, Accelerated spraying-assisted layer by layer assembly of polyethyleneimine/titanium nanosheet on thin film composite membrane for reverse osmosis desalination, *Desalination* 529 (2022) 115645.
- [23] N.N. Ahmad, A.W. Mohammad, E. Mahmoudi, W.L. Ang, C.P. Leo, Y.H. Teow, An overview of the modification strategies in developing antifouling nanofiltration membranes, *Membranes* 12 (12) (2022) 1276, <https://doi.org/10.3390/membranes12121276>.
- [24] C. Jiang, Z. Fei, M. Zhang, X. Ma, Y. Hou, Preparation of advanced reverse osmosis membrane by a wettability-transformable interlayer combining with N-acyl imidazole chemistry, *J. Membrane Sci.* 644 (2022) 120085.
- [25] C. Skuse, M. Alberto, J.M. Luque-Alled, V.O. Mercadillo, E. Asuquo, A. Gallego-Schmid, A. Azapagic, P. Gorgojo, Spray coating of 2D materials in the production of antifouling membranes for membrane distillation, *J. Membrane Sci.* 711 (2024) 123162.
- [26] Y.S. Khoo, W.J. Lau, Y.Y. Liang, B. Al-Maythaly, A.F. Ismail, Functionalization of reverse osmosis membrane with Titania nanotube and polyacrylic acid for enhanced antiscalting properties, *J. Environ. Chem. Eng.* 9 (5) (2021) 105937.
- [27] T. Sano, Y. Kawagoshi, I. Kokubo, H. Ito, K. Ishida, A. Sato, Direct and indirect effects of membrane pore size on fouling development in a submerged membrane bioreactor with a symmetric chlorinated poly (vinyl chloride) flat-sheet membrane, *J. Environ. Chem. Eng.* 10 (2) (2022) 107023.
- [28] D.G. Della Rocca, R.M. Peralta, R.A. Peralta, E. Rodríguez-Castellón, R. de Fatima Peralta Muniz Moreira, Adding value to aluminosilicate solid wastes to produce adsorbents, catalysts and filtration membranes for water and wastewater treatment, *J. Mater. Sci.* 56 (2) (2020) 1039–1063.
- [29] C.-M. Chow, R. Karnik, Effect of pore size distribution on the desalination performance of the selective layer of nanoporous atomically-thin membranes, *Desalination* 561 (2023) 116645.
- [30] A.R. Corcos, G.A. Levato, Z. Jiang, A.M. Evans, A.G. Livingston, B.J. Mariñas, W. R. Dichtel, Reducing the pore size of covalent organic frameworks in thin-film composite membranes enhances solute rejection, *ACS Materials Letters* 1 (4) (2019) 440–446.
- [31] N. Baig, A. Matin, M. Khan, M. Mansha, D. Anand, N. AlBalawi, A.M. Nzila, Reverse osmosis membranes functionalized with polyglycidol decorated hyperbranched copolymer exhibits superior filtration performance and improved fouling resistance, *J. Environ. Chem. Eng.* 10 (6) (2022) 108943.
- [32] H. Li, Y. Guo, C. Liu, Y. Zhou, X. Lin, F. Gao, Microbial deposition and growth on polyamide reverse osmosis membrane surfaces: mechanisms, impacts, and potential cures, *Desalination* 548 (2023) 116301.
- [33] C. Hobbs, J. Taylor, S. Hong, Effect of surface roughness on fouling of RO and NF membranes during filtration of a high organic surficial groundwater, *J. Water Supply Res. Technol. AQUA* 55 (7–8) (2006) 559–570.
- [34] Z. Yin, C. Yang, C. Long, A. Li, Influence of surface properties of RO membrane on membrane fouling for treating textile secondary effluent, *Environ. Sci. Pollut. Res.* 24 (19) (2017) 16253–16262.
- [35] V. Vatanpour, M. Esmaili, M.H. Farahani, Fouling reduction and retention increment of polyethersulfone nanofiltration membranes embedded by amine-functionalized multi-walled carbon nanotubes, *J. Membr. Sci.* 466 (2014) 70–81.
- [36] P. Zhao, B. Gao, Q. Yue, P. Liu, H.K. Shon, Fatty acid fouling of forward osmosis membrane: effects of pH, calcium, membrane orientation, initial permeate flux and foulant composition, *J. Environ. Sci.* 46 (2016) 55–62.
- [37] N.K. Khanzadeh, S. Rehman, J.A. Kharraz, M.U. Farid, M. Khatri, N. Hilal, A.K. An, Reverse osmosis membrane functionalized with aminated graphene oxide and polydopamine nanospheres plugging for enhanced NDMA rejection and antifouling performance, *Chemosphere* 338 (2023) 139557.
- [38] H. Mahdavi, A. Rahimi, Zwitterion functionalized graphene oxide/polyamide thin film nanocomposite membrane: towards improved anti-fouling performance for reverse osmosis, *Desalination* 433 (2018) 94–107.
- [39] J. Farahbakhsh, M. Delnavaz, V. Vatanpour, Investigation of raw and oxidized multiwalled carbon nanotubes in fabrication of reverse osmosis polyamide membranes for improvement in desalination and antifouling properties, *Desalination* 410 (2017) 1–9.
- [40] S. Seyyed Shahabi, N. Azizi, V. Vatanpour, N. Yousefimehr, Novel functionalized graphitic carbon nitride incorporated thin film nanocomposite membranes for high-performance reverse osmosis desalination, *Sep. Purif. Technol.* 235 (2020) 116134.
- [41] V. Vatanpour, S. Pazireh, S.A. Naziri Mehrabani, S. Feizpoor, A. Habibi-Yangjeh, I. Koyuncu, TiO<sub>2</sub>/cds modified thin-film nanocomposite polyamide membrane for simultaneous enhancement of antifouling and chlorine-resistance performance, *Desalination* 525 (2022) 115506.
- [42] V. Vatanpour, S. Pazireh, S.A. Naziri Mehrabani, S. Feizpoor, A. Habibi-Yangjeh, I. Koyuncu, TiO<sub>2</sub>/CDs modified thin-film nanocomposite polyamide membrane for simultaneous enhancement of antifouling and chlorine-resistance performance, *Desalination* 525 (November 2021) (2022) 115506, <https://doi.org/10.1016/j.desal.2021.115506>.
- [43] Y. Wang, X. Meng, H. Wu, S. Bian, Y. Tong, C. Gao, G. Zhu, Improving permeability and anti-fouling performance in reverse osmosis application of polyamide thin film nanocomposite membrane modified with functionalized carbon nanospheres, *Sep. Purif. Technol.* 270 (2021) 118828.
- [44] S. Bakhodaye Dehghanpour, F. Parviziyan, V. Vatanpour, The role of CuO/TS-1, ZnO/TS-1, and Fe<sub>2</sub>O<sub>3</sub>/TS-1 on the desalination performance and antifouling properties of thin-film nanocomposite reverse osmosis membranes, *Sep. Purif. Technol.* 302 (2022) 122083.
- [45] H. Huang, X. Wang, Y. Deng, J. Zhang, Highly permeable and durable mixed-matrix reverse osmosis membranes filled with cellulose nanofibers-hybridized Ti<sub>3</sub>C<sub>2</sub>T<sub>x</sub>, *Desalination* 551 (2023) 116412.
- [46] Alka, S. Yadav, P. Singh, P. Jain, Polymeric membranes as sustainable material for water desalination: a review, *Desalination and Water Treatment* 269 (2022) 1–20, <https://doi.org/10.5004/dwt.2022.28753>.
- [47] X. Du, Y. Shi, V. Jegatheesan, I.U. Haq, A review on the mechanism, impacts and control methods of membrane fouling in MBR system, *Membranes* 10 (2) (2020) 24.
- [48] M. Chen, S.G. Heijman, L.C. Rietveld, State-of-the-art ceramic membranes for oily wastewater treatment: modification and application, *Membranes* 11 (11) (2021) 888.
- [49] M. Oprea, S.I. Voicu, Cellulose acetate-based materials for water treatment in the context of circular economy, *Water* 15 (10) (2023) 1860.
- [50] S.H. Aladwani, M.A. Al-Obaidi, I.M. Mujtaba, Performance of reverse osmosis based desalination process using spiral wound membrane: sensitivity study of operating parameters under variable seawater conditions, *Cleaner Engineering and Technology* 5 (2021) 100284.
- [51] I. Shigidi, A.E. Anqi, A. Elkhaleefa, A. Mohamed, I.H. Ali, E.I. Brima, Temperature impact on reverse osmosis permeate flux in the remediation of hexavalent chromium, *Water* 14 (1) (2021) 44.
- [52] S. Fernandes, I.B. Gomes, L.C. Simões, M. Simões, Overview on the hydrodynamic conditions found in industrial systems and its impact in (bio)fouling formation, *Chem. Eng. J.* 418 (2021) 129348.
- [53] M.Y. Ashfaq, M.A. Al-Ghouti, D.A. Da'na, H. Qiblawey, N. Zouari, Investigating the effect of temperature on calcium sulfate scaling of reverse osmosis membranes using FTIR, SEM-EDX and multivariate analysis, *Sci. Total Environ.* 703 (2020) 134726.
- [54] M.Y. Ashfaq, M.A. Al-Ghouti, D.A. Da'na, H. Qiblawey, N. Zouari, Effect of concentration of calcium and sulfate ions on gypsum scaling of reverse osmosis membrane, mechanistic study, *J. Mater. Res. Technol.* 9 (6) (2020) 13459–13473.
- [55] F. Zhou, W. Wang, K. Li, W. Yang, J. Lee, B. Xie, B. Wu, H. Ren, S. Hong, M. Zhan, Controlling of irreversible fouling and mechanism in a hybrid ceramic membrane bioreactor (cmbr)-reverse osmosis (Ro) process for textile wastewater reclamation, *Desalination* 586 (2024) 117914, <https://doi.org/10.1016/j.desal.2024.117914>.
- [56] X. Fan, G. Wei, X. Quan, Carbon nanomaterial-based membranes for water and wastewater treatment under electrochemical assistance, *Environ. Sci. Nano* 10 (1) (2023) 11–40, <https://doi.org/10.1039/d2en00545j>.
- [57] L.H. Da-Silva-Correa, H. Smith, M.C. Thibodeau, B. Welsh, H.L. Buckley, The application of non-oxidizing biocides to prevent biofouling in reverse osmosis polyamide membrane systems: a review, *Journal of Water Supply: Research and Technology-Aqua* 71 (2) (2022) 261–292, <https://doi.org/10.2166/aqua.2022.118>.
- [58] M. Pranić, E.M. Kimani, P.M. Biesheuvel, S. Porada, Desalination of complex multi-ionic solutions by reverse osmosis at different pH values, temperatures, and compositions, *ACS Omega* 6 (30) (2021) 19946–19955.
- [59] M.R. Landsman, S. Rongpipi, G. Freychet, E. Gann, C. Jaye, D.F. Lawler, L.E. Katz, G.M. Su, Linking water quality, fouling layer composition, and performance of reverse osmosis membranes, *J. Membr. Sci.* 680 (2023) 121717.
- [60] E.M.V. Hoek, T.M. Weigand, A. Edalat, Reverse osmosis membrane biofouling: causes, consequences and countermeasures, *npj Clean Water* 5 (2022) 45, <https://doi.org/10.1038/s41545-022-00183-0>.
- [61] Y. Hu, K. Lu, F. Yan, Y. Shi, P. Yu, S. Yu, S. Li, C. Gao, Enhancing the performance of aromatic polyamide reverse osmosis membrane by surface modification via covalent attachment of polyvinyl alcohol (PVA), *J. Membr. Sci.* 501 (2016) 209–219.
- [62] Z. Hao, S. Zhao, Q. Li, Y. Wang, J. Zhang, Z. Wang, J. Wang, Reverse osmosis membranes with sulfonate and phosphate groups having excellent anti-scaling and anti-fouling properties, *Desalination* 509 (2021) 115076.
- [63] S. Lee, H.-J. Kim, M. Tian, G. Khang, H.-W. Kim, T.-H. Bae, J. Lee, Silk fibroin-coated polyamide thin-film composite membranes with anti-scaling properties, *Desalination* 546 (2023) 116195, <https://doi.org/10.1016/j.desal.2022.116195>.
- [64] S. Lee, H.-J. Kim, M. Tian, G. Khang, H.-W. Kim, T.-H. Bae, J. Lee, Silk fibroin-coated polyamide thin-film composite membranes with anti-scaling properties, *Desalination* 546 (2023) 116195.
- [65] Y. Zhang, Y. Wan, G. Pan, H. Shi, H. Yan, J. Xu, M. Guo, Z. Wang, Y. Liu, Surface modification of polyamide reverse osmosis membrane with sulfonated polyvinyl alcohol for antifouling, *Appl. Surf. Sci.* 419 (2017) 177–187.
- [66] Z. Yan, Y. Zhang, H. Yang, G. Fan, A. Ding, H. Liang, G. Li, N. Ren, B. Van der Bruggen, Mussel-inspired polydopamine modification of polymeric membranes for the application of water and wastewater treatment: a review, *Chem. Eng. Res. Des.* 157 (2020) 195–214.
- [67] D.L. Zhao, Q. Zhao, H. Lin, S.B. Chen, T.-S. Chung, Pressure-assisted polydopamine modification of thin-film composite reverse osmosis membranes for enhanced desalination and antifouling performance, *Desalination* 530 (2022) 115671.

- [72] J. Wang, H. Guo, X. Shi, Z. Yao, W. Qing, F. Liu, C.Y. Tang, Fast polydopamine coating on reverse osmosis membrane: process investigation and membrane performance study, *J. Colloid Interface Sci.* 535 (2019) 239–244.
- [73] Y.-F. Guan, C. Boo, X. Lu, X. Zhou, H.-Q. Yu, M. Elimelech, Surface functionalization of reverse osmosis membranes with sulfonic groups for simultaneous mitigation of silica scaling and organic fouling, *Water Res.* 185 (2020) 116203.
- [74] S.-H. Park, S.O. Hwang, T.-S. Kim, A. Cho, S.J. Kwon, K.T. Kim, H.-D. Park, J.-H. Lee, Triclosan-immobilized polyamide thin film composite membranes with enhanced biofouling resistance, *Appl. Surf. Sci.* 443 (2018) 458–466.
- [75] B. Cao, A. Ansari, X. Yi, D.F. Rodrigues, Y. Hu, Gypsum scale formation on graphene oxide modified reverse osmosis membrane, *J. Membr. Sci.* 552 (2018) 132–143.
- [76] X. Huang, K.L. Marsh, B.T. McVerry, E.M.V. Hoek, R.B. Kaner, Low-fouling antibacterial reverse osmosis membranes via surface grafting of graphene oxide, *ACS Appl. Mater. Interfaces* 8 (23) (2016) 14334–14338.
- [77] N.A. Ahmad, P.S. Goh, A.K. Zulhairun, A.F. Ismail, Antifouling property of oppositely charged titania nanosheet assembled on thin film composite reverse osmosis membrane for highly concentrated oily saline water treatment, *Membranes* 10 (9) (2020).
- [78] S.H. Park, S.H. Kim, S.J. Park, S. Ryoo, K. Woo, J.S. Lee, T.S. Kim, H.D. Park, H. Park, Y.I. Park, J. Cho, J.H. Lee, Direct incorporation of silver nanoparticles onto thin-film composite membranes via arc plasma deposition for enhanced antibacterial and permeation performance, *J. Membr. Sci.* 513 (2016) 226–235.
- [79] Z.C. Ng, W.J. Lau, A.F. Ismail, GO/PVA-integrated TFN RO membrane: exploring the effect of orientation switching between PA and GO/PVA and evaluating the GO loading impact, *Desalination* 496 (2020) 114538.
- [80] A. Ansari, J. Peña-Bahamonde, M. Wang, D.L. Shaffer, Y. Hu, D.F. Rodrigues, Polyacrylic acid-brushes tethered to graphene oxide membrane coating for scaling and biofouling mitigation on reverse osmosis membranes, *J. Membr. Sci.* 630 (2021) 119308.
- [81] F.I. Azmi, P.S. Goh, A.F. Ismail, N.A. Ahmad, M.N.Z. Abidin, Enhancing the antifouling and chlorine resistance capabilities of thin-film composite reverse osmosis via surface grafting of dipeptide, *React. Funct. Polym.* 192 (2023) 105708.
- [82] Q. Hu, Y. Yuan, Z. Wu, H. Lu, N. Li, H. Zhang, The effect of surficial function groups on the anti-fouling and anti-scaling performance of thin-film composite reverse osmosis membranes, *J. Membr. Sci.* 668 (2023) 121276, <https://doi.org/10.1016/j.memsci.2022.121276>.
- [84] Y. Wang, Z. Wang, X. Han, J. Wang, S. Wang, Improved flux and anti-biofouling performances of reverse osmosis membrane via surface layer-by-layer assembly, *J. Membr. Sci.* 539 (2017) 403–411.
- [85] S.Y. Wang, X.F. Sun, W.J. Gao, Y.F. Wang, B.B. Jiang, M.Z. Afzal, C. Song, S. G. Wang, Mitigation of membrane biofouling by D-amino acids: effect of bacterial cell-wall property and D-amino acid type, *Colloids Surf. B Biointerfaces* 164 (2018) 20–26, <https://doi.org/10.1016/j.colsurfb.2017.12.055>.
- [86] Y. Wang, Z. Wang, J. Wang, S. Wang, Triple antifouling strategies for reverse osmosis membrane biofouling control, *J. Membr. Sci.* 549 (2018) 495–506.
- [87] H. Xu, K. Xiao, X. Wang, S. Liang, C. Wei, X. Wen, X. Huang, Outlining the roles of membrane-foulant and foulant-foulant interactions in organic fouling during microfiltration and ultrafiltration: a mini-review, *Frontiers in Chemistry* 8 (2020).
- [88] P.H. Hermans, Principles of the mathematical treatment of constant-pressure filtration, *J. Soc. Chem. Ind.* 55 (1936) 1.
- [89] J. Hermia, Blocking filtration. Application to non-Newtonian fluids, in: *Mathematical Models and Design Methods in Solid-Liquid Separation*, Springer, 1985, pp. 83–89.
- [90] J.M. Ochando-Pulido, M.D. Víctor-Ortega, A. Martínez-Ferez, Membrane fouling insight during reverse osmosis purification of pretreated olive mill wastewater, *Sep. Purif. Technol.* 168 (2016) 177–187, <https://doi.org/10.1016/j.seppur.2016.05.024>.
- [91] X. Hao, S. Gao, J. Tian, S. Wang, H. Zhang, Y. Sun, W. Shi, F. Cui, New insights into the organic fouling mechanism of an: in situ Ca<sup>2+</sup>-modified thin film composite forward osmosis membrane, *RSC Adv.* 9 (65) (2019) 38227–38234, <https://doi.org/10.1039/c9ra06272f>.
- [92] X. Meng, W. Tang, L. Wang, X. Wang, D. Huang, H. Chen, N. Zhang, Mechanism analysis of membrane fouling behavior by humic acid using atomic force microscopy: effect of solution pH and hydrophilicity of PVDF ultrafiltration membrane interface, *J. Membr. Sci.* 487 (2015) 180–188, <https://doi.org/10.1016/j.memsci.2015.03.034>.
- [93] T.V. Nguyen, M.T.M. Pendergast, M.T. Phong, X. Jin, F. Peng, M.L. Lind, E.M. V. Hoek, Relating fouling behavior and cake layer formation of alginate acid to the physicochemical properties of thin film composite and nanocomposite seawater RO membranes, *Desalination* 338 (1) (2014) 1–9, <https://doi.org/10.1016/j.desal.2014.01.013>.
- [94] Z. Liang, Y. Yun, Q. Ji, Q. Xia, C. Li, Effects of organic solvents and different aqueous-phase additives on the polyamide (PA) thin-film composite (TFC) membranes for forward osmosis, *Desalin. Water Treat.* 119 (2018) 44–52, <https://doi.org/10.5004/dwt.2018.22075>.
- [95] C.J. van Oss, Development and applications of the interfacial tension between water and organic or biological surfaces, *Colloids Surf. B Biointerfaces* 54 (1) (2007) 2–9, <https://doi.org/10.1016/j.colsurfb.2006.05.024>.
- [96] H. Jaramillo, C. Boo, S.M. Hashmi, M. Elimelech, Zwitterionic coating on thin-film composite membranes to delay gypsum scaling in reverse osmosis, *J. Membr. Sci.* 618 (2021) 118568, <https://doi.org/10.1016/j.memsci.2020.118568>.
- [97] L. Hu, H. Lu, X. Ma, X. Chen, Heterogeneous nucleation on surfaces of the three-dimensional cylindrical substrate, *J. Cryst. Growth* 575 (2021) 126340, <https://doi.org/10.1016/j.jcrysgro.2021.126340>.
- [98] M. Förster, M. Bohnet, Influence of the interfacial free energy crystal/heat transfer surface on the induction period during fouling, *Int. J. Therm. Sci.* 38 (11) (1999) 944–954, [https://doi.org/10.1016/S1290-0729\(99\)00102-7](https://doi.org/10.1016/S1290-0729(99)00102-7).
- [99] C. Dong, Z. Wang, J. Wu, Y. Wang, J. Wang, S. Wang, A green strategy to immobilize silver nanoparticles onto reverse osmosis membrane for enhanced anti-biofouling property, *Desalination* 401 (2017) 32–41, <https://doi.org/10.1016/j.desal.2016.06.034>.
- [101] Y. Jung, S. Lee, K. Kim, T.H. Bae, J. Lee, Silk sericin-coated polyamide thin-film composite membranes to simultaneously improve anti-scaling properties, long-term storage, and waste-to-resource recovery, *Desalination* 591 (July) (2024) 118015, <https://doi.org/10.1016/j.desal.2024.118015>.
- [102] F. Seyedpour, J. Farahbakhsh, Z. Dabaghian, W. Suwaileh, M. Zargar, A. Rahimpour, M. Sadrzadeh, M. Ulbricht, Y. Mansourpanah, Advances and challenges in tailoring antibacterial polyamide thin film composite membranes for water treatment and desalination: a critical review, *Desalination* 581 (2024) 117614, <https://doi.org/10.1016/j.desal.2024.117614>.
- [103] X. Qian, J. Huang, X. Ji, C. Yan, C. Cao, Y. Wu, X. Wang, Modified basalt fibers boost performance of constructed wetlands: comparison between surface coating and chemical grafting, *Bioresour. Technol.* 397 (2024) 130492, <https://doi.org/10.1016/j.biortech.2024.130492>.
- [104] G. Li, L. Liu, J. Luo, J. Guo, L. Chen, Y. Wan, X. Chen, Enhancing silica scaling resistance of high-pressure reverse osmosis membranes through surface grafting with various sulfonic acid monomers, *Desalination* 591 (July) (2024) 118028, <https://doi.org/10.1016/j.desal.2024.118028>.
- [105] J. Ayyavoo, T.P.N. Nguyen, B.M. Jun, I.C. Kim, Y.N. Kwon, Protection of polymeric membranes with antifouling surfacing via surface modifications, *Colloids Surf. A Physicochem. Eng. Asp.* 506 (2016) 190–201, <https://doi.org/10.1016/j.colsurfa.2016.06.026>.
- [106] Q. Zhang, R. Zhou, X. Peng, N. Li, Z. Dai, Development of support layers and their impact on the performance of thin film composite membranes (TFC) for water treatment, *Polymers* 15 (15) (2023) 3290, <https://doi.org/10.3390/polym15153290>.
- [107] F. Shao, C. Xu, W. Ji, H. Dong, Q. Sun, L. Yu, L. Dong, Layer-by-layer self-assembly TiO<sub>2</sub> and graphene oxide on polyamide reverse osmosis membranes with improved membrane durability, *Desalination* 423 (2017) 21–29, <https://doi.org/10.1016/j.desal.2017.09.007>.
- [108] J. Chen, S. Xu, C.Y. Tang, B. Hu, B. Tokay, T. He, Stability of layer-by-layer nanofiltration membranes in highly saline streams, *Desalination* 555 (2023) 116520, <https://doi.org/10.1016/j.desal.2023.116520>.
- [109] Z. Yang, P.-F. Sun, X. Li, B. Gan, L. Wang, X. Song, H.-D. Park, C.Y. Tang, A critical review on thin-film nanocomposite membranes with interlayered structure: mechanisms, recent developments, and environmental applications, *Environ. Sci. Technol.* 54 (24) (2020) 15563–15583, <https://doi.org/10.1021/acs.est.0c05377>.
- [110] Y. Zhang, Y. Wan, M. Guo, G. Pan, H. Shi, X. Yao, Y. Liu, Surface modification on thin-film composite reverse osmosis membrane by cation complexation for antifouling, *J. Polym. Res.* 26 (3) (2019) 68, <http://link.springer.com/10.1007/s10965-019-1701-0>.
- [111] C.S. Lee, I. Kim, J.W. Jang, D. sung Yoon, Y.J. Lee, Aquaporin-incorporated graphene-oxide membrane for pressurized desalination with superior integrity enabled by molecular recognition, *Adv. Sci.* 8 (20) (2021) 1–10, <https://doi.org/10.1002/adv.202101882>.
- [112] A. hameed M.A. El-Aassar, Improvement of reverse osmosis performance of polyamide thin-film composite membranes using TiO<sub>2</sub> nanoparticles, *Desalination and Water Treatment* 55 (11) (2015) 2939–2950, <https://doi.org/10.1080/19443994.2014.940206>.
- [113] B. Bolto, Z. Xie, Recent developments in fouling minimization of membranes modified with silver nanoparticles, *Journal of Membrane Science and Research* 4 (3) (2018) 111–120, <https://doi.org/10.22079/JMSR.2018.79056.1168>.
- [114] N.S.M. Nawi, W.J. Lau, P.S. Goh, J.W. Chew, S. Gray, N. Yusof, A.F. Ismail, The impacts of 2D graphene oxide on selective and substrate layer of TFC membrane: a critical review on fabrication techniques and performance in water treatment, *J. Environ. Chem. Eng.* 12 (2) (2024) 112298, <https://doi.org/10.1016/j.jece.2024.112298>.
- [115] L.Y. Ng, A.W. Mohammad, C.P. Leo, N. Hilal, Polymeric membranes incorporated with metal/metal oxide nanoparticles: a comprehensive review, *Desalination* 308 (2013) 15–33, <https://doi.org/10.1016/j.desal.2010.11.033>.
- [160] X. Gao, Y. Li, X. Yang, Y. Shang, Y. Wang, B. Gao, Highly permeable and antifouling reverse osmosis membranes with acidified graphitic carbon nitride nanosheets as nanofillers, *J. Mater. Chem.* 5 (2017) 19875–19883.
- [162] D. Chen, Q. Chen, T. Liu, J. Kang, R. Xu, Y. Cao, M. Xiang, Influence of l-arginine on performances of polyamide thin-film composite reverse osmosis membranes, *RSC Adv.* 9 (35) (2019) 20149–20160.
- [163] D. Chen, R. Hu, Y. Song, F. Gao, W. Peng, Y. Zhang, Z. Xie, J. Kang, Z. Zheng, Y. Cao, M. Xiang, Hydrophilic modified polydopamine tailored heterogeneous polyamide in thin-film nanocomposite membranes for enhanced separation performance and anti-fouling properties, *J. Membr. Sci.* 666 (2023) 121124.
- [164] F. Asempour, D. Emadzadeh, T. Matsuura, B. Kruczek, Synthesis and characterization of novel Cellulose Nanocrystals-based Thin Film Nanocomposite membranes for reverse osmosis applications, *Desalination* 439 (2018) 179–187.
- [165] Z. Liao, X. Fang, J. Li, X. Li, W. Zhang, X. Sun, J. Shen, W. Han, S. Zhao, L. Wang, Incorporating organic nanospheres into the polyamide layer to prepare thin film composite membrane with enhanced biocidal activity and chlorine resistance,

- Sep. Purif. Technol. 207 (2018) 222–230, <https://doi.org/10.1016/j.seppur.2018.06.057>.
- [166] S.J. Park, M.S. Lee, H. Yoon, J.H. Kim, S. Jeon, S.S. Shin, M. Yang, J. Choi, J. Seo, J.H. Lee, Biomimetic peptoid-assisted fabrication of antibiofouling thin-film composite membranes, *Chem. Eng. J.* 478 (2023) 147468.
- [167] Z. Fei, C. Jiang, M. Li, Y. Hou, Imidazole assisted molecular-scale regulation of polyamide for preparing reverse osmosis membrane with enhanced water permeance, *J. Environ. Chem. Eng.* 10 (2022) 108146, <https://doi.org/10.1016/j.jece.2022.108146>.
- [168] Y. Wang, H. Xu, M. Ding, L. Zhang, G. Chen, J. Fu, A. Wang, J. Chen, B. Liu, W. Yang, MXene-regulation polyamide membrane featuring with bubble-like module for efficient dye/salt separation and antifouling performance, *RSC Adv.* 12 (17) (2022) 10267–10279.
- [169] Y. Li, S. Yang, K. Zhang, B. Van der Bruggen, Thin film nanocomposite reverse osmosis membrane modified by two dimensional laminar MoS<sub>2</sub> with improved desalination performance and fouling-resistant characteristics, *Desalination* 454 (2019) 48–58, <https://doi.org/10.1016/j.desal.2018.12.016>.
- [170] X. Wang, Q. Li, J. Zhang, H. Huang, S. Wu, Y. Yang, Novel thin-film reverse osmosis membrane with MXene Ti<sub>3</sub>C<sub>2</sub>Tx embedded in polyamide to enhance the water flux, anti-fouling and chlorine resistance for water desalination, *J. Membr. Sci.* 603 (2020) 118036, <https://doi.org/10.1016/j.memsci.2020.118036>.
- [171] P.S. Goh, W.J. Lau, M.H.D. Othman, A.F. Ismail, Membrane fouling in desalination and its mitigation strategies, *Desalination* 425 (2018) 130–155, <https://doi.org/10.1016/j.desal.2017.10.018>.
- [172] R. Wang, Z.X. Low, S. Liu, Y. Wang, S. Murthy, W. Shen, H. Wang, Thin-film composite polyamide membrane modified by embedding functionalized boron nitride nanosheets for reverse osmosis, *J. Membr. Sci.* 611 (2020) 118389.
- [174] M. Ge, Z. Jia, Y. Yang, P. Dong, C. Peng, X. Zhang, R. Dewil, Y. Zhao, B. Van der Bruggen, J. Zhang, In situ assembly of graphitic carbon nitride/polypyrrole in a thin-film nanocomposite membrane with highly enhanced permeability and durability, *Desalination* 555 (2023) 116566, <https://doi.org/10.1016/j.desal.2023.116566>.
- [175] D. Suresh, P.S. Goh, A.F. Ismail, S.B. Mansur, K.C. Wong, M.H. Asraf, N.A.N. N. Malek, T.W. Wong, Complexation of tannic acid/silver nanoparticles on polyamide thin film composite reverse osmosis membrane for enhanced chlorine resistance and anti-biofouling properties, *Desalination* 543 (2022) 116107, <https://doi.org/10.1016/j.desal.2022.116107>.
- [177] J. Zhu, J. Hou, Y. Zhang, M. Tian, T. He, J. Liu, V. Chen, Polymeric antimicrobial membranes enabled by nanomaterials for water treatment, *J. Membr. Sci.* 550 (2018) 173–197, <https://doi.org/10.1016/j.memsci.2017.12.071>.
- [178] H. Isawi, Synthesis of graphene oxide-silver (GO-Ag) nanocomposite TFC RO membrane to enhance morphology and separation performances for groundwater desalination, (case study Marsa Alam area- Red Sea), *Chem. Eng. Process. - Process Intensif.* 187 (2023) 109343, <https://doi.org/10.1016/j.ccep.2023.109343>.
- [179] J. Zhu, J. Wang, A.A. Uliana, M. Tian, Y. Zhang, Y. Zhang, A. Volodin, K. Simoens, S. Yuan, J. Li, J. Lin, K. Bernaerts, B. Van der Bruggen, Mussel-Inspired Architecture of High-Flux Loose Nanofiltration Membrane Functionalized with Antibacterial Reduced Graphene Oxide–Copper Nanocomposites, *ACS Appl. Mater. Interfaces* 9 (2017) 28990–29001, <https://doi.org/10.1021/acsami.7b05930>.
- [181] N. Li, L. Yu, Z. Xiao, C. Jiang, B. Gao, Z. Wang, Biofouling mitigation effect of thin film nanocomposite membranes immobilized with laponite mediated metal ions, *Desalination* 473 (2020) 114162, <https://doi.org/10.1016/j.desal.2019.114162>.
- [183] M.U. Shahid, T. Najam, M. Islam, A.M. Hassan, M.A. Assiri, A. Rauf, A. ur Rehman, S.S.A. Shah, M.A. Nazir, Engineering of metal organic framework (MOF) membrane for waste water treatment: Synthesis, applications and future challenges, *J. Water Process Eng.* 57 (2024) 104676, <https://doi.org/10.1016/j.jwpe.2023.104676>.
- [184] Y. Liu, X.P. Wang, Z.A. Zong, R.J. Lin, X.Y. Zhang, F.S. Chen, W.D. Ding, L. L. Zhang, X.M. Meng, J.W. Hou, Thin film nanocomposite membrane incorporated with 2D-MOF nanosheets for highly efficient reverse osmosis desalination, *J. Membr. Sci.* 653 (2022) 120520.
- [185] I.H. Aljundi, Desalination characteristics of TFN-RO membrane incorporated with ZIF-8 nanoparticles, *Desalination* 420 (2017) 12–20, <https://doi.org/10.1016/j.desal.2017.06.020>.
- [186] X. Dong, X. Wang, H. Xu, Y. Huang, C. Gao, X. Gao, Mesoporous hollow nanospheres with amino groups for reverse osmosis membranes with enhanced permeability, *J. Membr. Sci.* 657 (2022) 120637, <https://doi.org/10.1016/j.memsci.2022.120637>.
- [187] C. Chen, Y. Yang, N.J.D. Graham, Z. Li, X. Yang, Z. Wang, N. Farhat, J. S. Vrouwenvelder, L.A. Hou, A comprehensive evaluation of the temporal and spatial fouling characteristics of RO membranes in a full-scale seawater desalination plant, *Water Res.* 249 (2024) 120914, <https://doi.org/10.1016/j.watres.2023.120914>.
- [188] Y. Du, X. Zhang, C. Cao, J. Dai, Q. Gong, D. Zhang, H. Deng, L. Xie, Optimal design and operation of reverse osmosis seawater desalination system for boron removal with economic, energy, and environmental concerns, *Desalination* 2023 (546) (2023) 116178.
- [191] Y. Lester, A. Hazut, A. Spanier, Formation of Organic Fouling during Membrane Desalination: The Effect of Divalent Cations and the Use of an Online Visual Monitoring Method, *Membranes (Basel)* 23 (12) (2022) 1177, <https://doi.org/10.3390/membranes12121177>.